Mars Atmosphere and Volatile Evolution (MAVEN) Mission

Solar Wind Electron Analyzer (SWEA)

PDS Archive

Software Interface Specification

Rev. 2.4

SWEA

May 29, 2015

Prepared by

David L. Mitchell

mitchell@ssl.berkeley.edu

MAVEN

Solar Wind Electron Analyzer (SWEA)

PDS Archive

Software Interface Specification

Rev. 2.4 SWEA

May 29, 2015

Custodian:

David L. Mitchell	Date
SWEA Principal Investigator	

Approved:

Alexandria DeWolfe	Date
MAVEN Science Data Center Lead	
Raymond J. Walker	Date
PDS PPI Node Manager	
Thomas H. Morgan	Date
PDS Project Manager	

Contents

List of Figures

List of Tables

Introduction

This software interface specification (SIS) describes the format and content of the Solar Wind Electron Analyzer (SWEA) Planetary Data System (PDS) data archive. It includes descriptions of the data products and associated metadata, and the archive format, content, and generation pipeline.

1.1 Distribution List

Table 1: Distribution list

Name	Organization	Email
David L. Mitchell	UCB/SSL	mitchell@ssl.berkeley.edu
Alexandria DeWolfe	LASP/SDC	alex.dewolfe@lasp.colorado.edu
Steve Joy	UCLA/PDS/PPI	sjoy@igpp.ucla.edu
Ray Walker	UCLA/PDS/PPI	rwalker@igpp.ucla.edu
Joe Mafi	UCLA/PDS/PPI	jmafi@igpp.ucla.edu
Reta Beebe	NMSU/PDS/Atmospheres	
Lyle Huber	NMSU/PDS/Atmospheres	
Lynn Neakrase	NMSU/PDS/Atmospheres	

1.2 Document Change Log

Table 2: Document change log

Version	Change	Date	Affected portion
0.0	Initial template	2012-Aug-24	All
0.1	Updated template	2013-Feb-13	All
0.2	Updated template	2013-Apr-03	All
0.3	Updated template	2014-Jan-30	All
0.4	Updated for SWEA	2014-Mar-05	All
1.0	Signature Version	2014-Mar-27	All
2.0	Updated following peer review	2014-Sep-08	All
2.1	More revisions and formatting	2014-Oct-06	All
2.2	More revisions and formatting	2014-Oct-29	All
2.3	Minor revisions and corrections	2014-Oct-31	All
2.4	Additional explanation of data as requested at the peer review	2015-May-29	Section 5.2

1.3 TBD Items

Table 3 lists items that are not yet finalized.

Table 3: List of TBD items

Item	Section(s)	Page(s)
Full references for PDS4 Standards Reference, and Data Provider's Handbook documents (to be provided by PDS/PPI)	1.9	8
Sample labels (to be provided by PDS/PPI)	Appendices C, D, and E	49-51

1.4 Abbreviations

Table 4: Abbreviations and their meaning

Abbreviation	Meaning
ASCII	American Standard Code for Information Interchange
Atmos	PDS Atmospheres Node (NMSU, Las Cruces, NM)
CCSDS	Consultative Committee for Space Data Systems
CDF	Common Data Format
CDR	Calibrated Data Record
CFDP	CCSDS File Delivery Protocol
CK	C-matrix Kernel (NAIF orientation data)
CODMAC	Committee on Data Management, Archiving, and Computing
CRC	Cyclic Redundancy Check
CU	University of Colorado (Boulder, CO)
DAP	Data Analysis Product
DDR	Derived Data Record
DMAS	Data Management and Storage
DPF	Data Processing Facility
E&PO	Education and Public Outreach
EDR	Experiment Data Record
EUV	Extreme Ultraviolet; also used for the EUV Monitor, part of LPW (SSL)
FEI	File Exchange Interface
FOV	Field of View
FTP	File Transfer Protocol

Abbreviation	Meaning
GB	Gigabyte(s)
GSFC	Goddard Space Flight Center (Greenbelt, MD)
HK	Housekeeping
HTML	Hypertext Markup Language
ICD	Interface Control Document
IDL	Interactive Data Language
IM	Information Model
ISO	International Standards Organization
IRAP	Institut de Recherche en Astrophysique et Planétologie
ITF	Instrument Team Facility
IUVS	Imaging Ultraviolet Spectrograph (LASP)
JPL	Jet Propulsion Laboratory (Pasadena, CA)
LASP	Laboratory for Atmosphere and Space Physics (CU)
LID	Logical Identifier
LIDVID	Versioned Logical Identifer
LPW	Langmuir Probe and Waves instrument (SSL)
MAG	Magnetometer instrument (GSFC)
MAVEN	Mars Atmosphere and Volatile EvolutioN
MET	Mission Elapsed Time
MB	Megabyte(s)
MCP	Microchannel Plate
MD5	Message-Digest Algorithm 5
MOI	Mars Orbit Insertion
MOS	Mission Operations System
MSA	Mission Support Area
NAIF	Navigation and Ancillary Information Facility (JPL)
NASA	National Aeronautics and Space Administration
NGIMS	Neutral Gas and Ion Mass Spectrometer (GSFC)
NMSU	New Mexico State University (Las Cruces, NM)
NSSDC	National Space Science Data Center (GSFC)

Abbreviation	Meaning
PAD	Pitch Angle Distribution
PCK	Planetary Constants Kernel (NAIF)
PDS	Planetary Data System
PDS4	Planetary Data System Version 4
PF	Particles and Fields (instruments)
PFDPU	Particles and Fields Data Processing Unit
POC	Payload Operations Center
PPI	PDS Planetary Plasma Interactions Node (UCLA)
RS	Remote Sensing (instruments)
SCET	Spacecraft Event Time
SCLK	Spacecraft Clock
SDC	Science Data Center (LASP)
SEP	Solar Energetic Particle instrument (SSL)
SIS	Software Interface Specification
SOC	Science Operations Center (LASP)
SPE	Solar Particle Event
SPICE	Spacecraft, Planet, Instrument, C-matrix, and Events (NAIF data format)
SPK	Spacecraft and Planetary ephemeris Kernel (NAIF)
SSL	Space Sciences Laboratory (UCB)
STATIC	Supra-Thermal And Thermal Ion Composition instrument (SSL)
SWEA	Solar Wind Electron Analyzer (SSL)
SWIA	Solar Wind Ion Analyzer (SSL)
TBC	To Be Confirmed
TBD	To Be Determined
UCB	University of California, Berkeley
UCLA	University of California, Los Angeles
URN	Uniform Resource Name
UV	Ultraviolet
VID	1.4.1.1.1.1 Versioned Logical Identifier
XML	eXtensible Markup Language

1.5 Glossary

Archive – A place in which public records or historical documents are preserved; also the material preserved – often used in plural. The term may be capitalized when referring to all of PDS holdings – the PDS Archive.

Basic Product – The simplest product in PDS4; one or more data objects (and their description objects), which constitute (typically) a single observation, document, etc. The only PDS4 products that are *not* basic products are collection and bundle products.

Bundle Product – A list of related collections. For example, a bundle could list a collection of raw data obtained by an instrument during its mission lifetime, a collection of the calibration products associated with the instrument, and a collection of all documentation relevant to the first two collections.

Class – The set of attributes (including a name and identifier) which describes an item defined in the PDS Information Model. A class is generic – a template from which individual items may be constructed.

Collection Product – A list of closely related basic products of a single type (e.g. observational data, browse, documents, etc.). A collection is itself a product (because it is simply a list, with its label), but it is not a *basic* product.

Data Object – A generic term for an object that is described by a description object. Data objects include both digital and non-digital objects.

Description Object – An object that describes another object. As appropriate, it will have structural and descriptive components. In PDS4 a 'description object' is a digital object – a string of bits with a predefined structure.

Digital Object – An object which consists of real electronically stored (digital) data.

Identifier – A unique character string by which a product, object, or other entity may be identified and located. Identifiers can be global, in which case they are unique across all of PDS (and its federation partners). A local identifier must be unique within a label.

Label – The aggregation of one or more description objects such that the aggregation describes a single PDS product. In the PDS4 implementation, labels are constructed using XML.

Logical Identifier (LID) – An identifier which identifies the set of all versions of a product.

Versioned Logical Identifier (LIDVID) – The concatenation of a logical identifier with a version identifier, providing a unique identifier for each version of product.

Manifest - A list of contents.

Metadata – Data about data – for example, a 'description object' contains information (metadata) about an 'object.'

Non-Digital Object – An object which does not consist of digital data. Non-digital objects include both physical objects like instruments, spacecraft, and planets, and non-physical objects like missions, and institutions. Non-digital objects are labeled in PDS in order to define a unique identifier (LID) by which they may be referenced across the system.

Object – A single instance of a class defined in the PDS Information Model.

PDS Information Model – The set of rules governing the structure and content of PDS metadata. While the Information Model (IM) has been implemented in XML for PDS4, the model itself is implementation independent.

Product – One or more tagged objects (digital, non-digital, or both) grouped together and having a single PDS-unique identifier. In the PDS4 implementation, the descriptions are combined into a single XML label. Although it may be possible to locate individual objects within PDS (and to find specific bit strings within digital objects), PDS4 defines 'products' to be the smallest granular unit of addressable data within its complete holdings.

Tagged Object – An entity categorized by the PDS Information Model, and described by a PDS label.

Registry – A data base that provides services for sharing content and metadata.

Repository – A place, room, or container where something is deposited or stored (often for safety).

XML – eXtensible Markup Language.

XML schema – The definition of an XML document, specifying required and optional XML elements, their order, and parent-child relationships.

1.6 MAVEN Mission Overview

The MAVEN mission is scheduled to launch on an Atlas V between November 18 and December 7, 2013. After a ten-month ballistic cruise phase, Mars orbit insertion will occur on or after September 22, 2014. Following a 5-week transition phase, the spacecraft will orbit Mars at a 75° inclination, with a 4.5 hour period and periapsis altitude of 140-170 km (density corridor of 0.05-0.15 kg/km^3). Over a one-Earth-year period, periapsis will precess over a wide range of latitude and local time, while MAVEN obtains detailed measurements of the upper atmosphere, ionosphere, planetary corona, solar wind, interplanetary/Mars magnetic fields, solar EUV and solar energetic particles, thus defining the interactions between the Sun and Mars. MAVEN will explore down to the homopause during a series of five 5-day "deep dip" campaigns for which periapsis will be lowered to an atmospheric density of 2 kg/km^3 (~125 km altitude) in order to sample the transition from the collisional lower atmosphere to the collisionless upper atmosphere. These five campaigns will be interspersed though the mission to sample the subsolar region, the dawn and dusk terminators, the anti-solar region, and the north pole.

1.6.1 Mission Objectives

The primary science objectives of the MAVEN project will be to provide a comprehensive picture of the present state of the upper atmosphere and ionosphere of Mars and the processes controlling them and to determine how loss of volatiles to outer space in the present epoch varies with changing solar conditions. Knowing how these processes respond to the Sun's energy inputs will enable scientists, for the first time, to reliably project processes backward in time to study atmosphere and volatile evolution. MAVEN will deliver definitive answers to high-priority science questions about atmospheric loss (including water) to space that will greatly enhance our understanding of the climate history of Mars. Measurements made by MAVEN will allow us to determine the role that escape to space has played in the evolution of the Mars atmosphere, an essential component of the quest to "follow the water" on Mars. MAVEN will accomplish this by achieving science objectives that answer three key science questions:

- What is the current state of the upper atmosphere and what processes control it?
- What is the escape rate at the present epoch and how does it relate to the controlling processes?
- What has the total loss to space been through time?

MAVEN will achieve these objectives by measuring the structure, composition, and variability of the Martian upper atmosphere, and it will separate the roles of different loss mechanisms for both neutrals and ions. MAVEN will sample all relevant regions of the Martian atmosphere/ionosphere system—from the termination of the well-mixed portion of the atmosphere (the "homopause"), through the diffusive region and main ionosphere layer, up into the collisionless exosphere, and through the magnetosphere and into the solar wind and downstream tail of the planet where loss of neutrals and ionization occurs to space—at all relevant latitudes and local solar times. To allow a meaningful projection of escape back in time, measurements of escaping species will be made simultaneously with measurements of the energy drivers and the controlling magnetic field over a range of solar conditions. Together with measurements of the isotope ratios of major species, which constrain the net loss to space over time, this approach will allow thorough identification of the role that atmospheric escape plays today and to extrapolate to earlier epochs.

1.6.2 Payload

MAVEN will use the following science instruments to measure the Martian upper atmospheric and ionospheric properties, the magnetic field environment, the solar wind, and solar radiation and particle inputs:

- NGIMS Package:
  - Neutral Gas and Ion Mass Spectrometer (NGIMS) measures the composition, isotope ratios, and scale heights of thermal ions and neutrals.
- RS Package:
  - Imaging Ultraviolet Spectrograph (IUVS) remotely measures UV spectra in four modes: limb scans, planetary mapping, coronal mapping and stellar occultations. These measurements provide the global composition, isotope ratios, and structure of the upper atmosphere, ionosphere, and corona.
- PF Package:

- Supra-Thermal and Thermal Ion Composition (STATIC) instrument measures the velocity distributions and mass composition of thermal and suprathermal ions from below escape energy to pickup ion energies.
- Solar Energetic Particle (SEP) instrument measures the energy spectrum and angular distribution of solar energetic electrons (30 keV – 1 MeV) and ions (30 keV – 12 MeV).
- Solar Wind Ion Analyzer (SWIA) measures solar wind and magnetosheath ion density, temperature, and bulk flow velocity. These measurements are used to determine the charge exchange rate and the solar wind dynamic pressure.
- Solar Wind Electron Analyzer (SWEA) measures energy and angular distributions of 5 eV to 5 keV solar wind, magnetosheath, and auroral electrons, as well as ionospheric photoelectrons. These measurements are used to constrain the plasma environment, magnetic field topology and electron impact ionization rate.
- Langmuir Probe and Waves (LPW) instrument measures the electron density and temperature and electric field in the Mars environment. The instrument includes an EUV Monitor that measures the EUV input into Mars atmosphere in three broadband energy channels.
- Magnetometer (MAG) measures the vector magnetic field in all regions traversed by MAVEN in its orbit.

1.7 SIS Content Overview

Section 2 describes the SWEA instrument. Section 3 gives an overview of data organization and data flow. Section 4 describes data archive generation, delivery, and validation. Section 5 describes the archive structure and archive production responsibilities. Section 6 describes the file formats used in the archive, including the data product record structures. Individuals involved with generating the archive volumes are listed in Appendix A. Appendix B contains a description of the MAVEN science data file naming conventions. Appendix C, Appendix D, and Appendix E contain sample PDS product labels. Appendix F describes SWEA archive product PDS deliveries formats and conventions.

1.8 Scope of this document

The specifications in this SIS apply to all SWEA products submitted for archive to the Planetary Data System (PDS), for all phases of the MAVEN mission. This document includes descriptions of archive products that are produced by both the SWEA team and by PDS.

1.9 Applicable Documents

[1] Planetary Data System Data Provider's Handbook, TBD.

[2] Planetary Data System Standards Reference, TBD.

[3] PDS4 Data Dictionary – Abridged, Version 1.1.0.1, 21 November 2013.

[4] Planetary Data System (PDS) PDS4 Information Model Specification, Version 1.1.0.1.

[5] Mars Atmosphere and Volatile Evolution (MAVEN) Science Data Management Plan, Rev. C, doc. no.MAVEN-SOPS-PLAN-0068.

[6] King, T., and J. Mafi, Archive of MAVEN CDF in PDS4, July 16, 2013.

1.10 Audience

This document serves both as a SIS and Interface Control Document (ICD). It describes both the archiving procedure and responsibilities, and data archive conventions and format. It is designed to be used both by the instrument teams in generating the archive, and by those wishing to understand the format and content of the SWEA PDS data product archive collection. Typically, these individuals would include scientists, data analysts, and software engineers.

2 SWEA Instrument Description

The Solar Wind Electron Analyzer (SWEA) is a symmetric, hemispheric electrostatic analyzer designed to measure the energy and angular distributions of solar wind electrons and ionospheric photoelectrons in the Mars environment (**Error! Reference source not found.**). The instrument is a collaboration between the Space Sciences Laboratory at the University of California, Berkeley (UCB-SSL) and the Institut de Recherche en Astrophysique et Planétologie (IRAP) in Toulouse, France. SWEA is closely based on two instruments of the same name currently operating on the twin STEREO spacecraft (Sauvaud et al., 2008). For MAVEN, IRAP provided the analyzer and front-end electronics (microchannel plates, anode, preamplifiers, and high voltage power supply), while UCB-SSL provided the low voltage power supply and digital electronics, which controls the analyzer operation and interfaces with the Particles and Fields Data Processing Unit (PFDPU). SWEA data products are calculated by software in the PFDPU and placed into the telemetry stream for transmission to the ground.

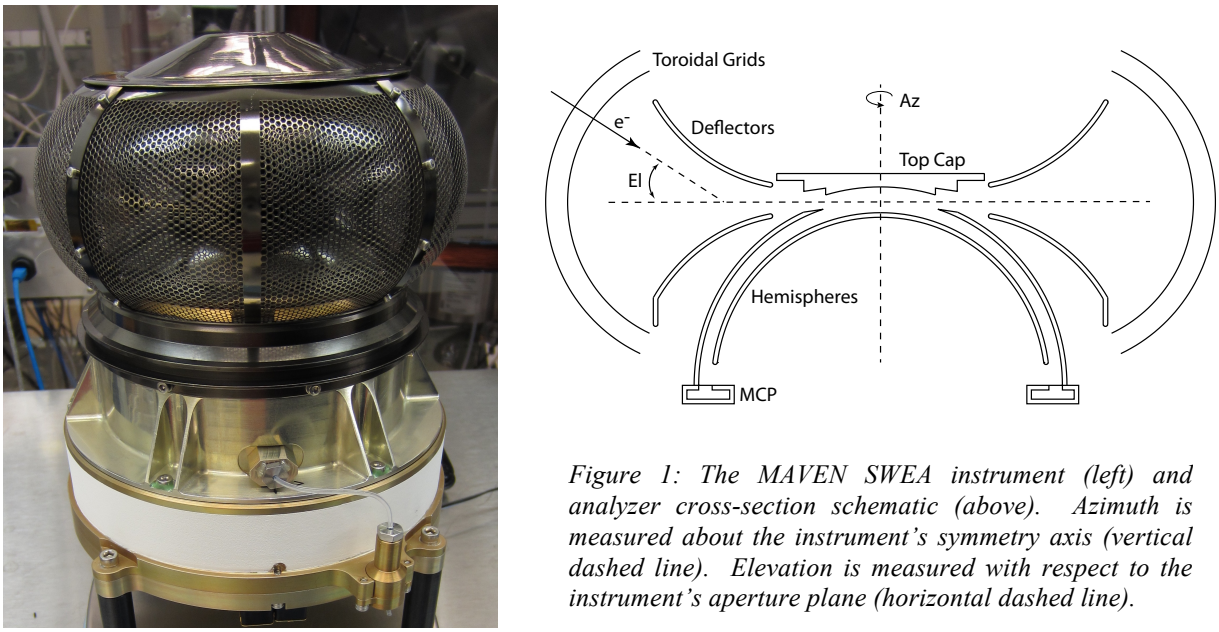

Figure 1: The MAVEN SWEA instrument (left) and analyzer cross-section schematic (above). Azimuth is measured about the instrument's symmetry axis (vertical dashed line). Elevation is measured with respect to the instrument's aperture plane (horizontal dashed line).

SWEA selects electrons within a given energy range by placing a potential difference between two concentric hemispheres. Electrons that pass through this analyzer are incident on a chevron pair of microchannel plates (MCPs) that amplify the signal by a factor of ~10^6. The resulting electron cloud lands on a charge collecting anode that is segmented into 16 equal sized sectors, providing 22.5° azimuth resolution. The charge pulse on each anode sector is detected by one of 16 preamplifiers, which provide signals that are counted by a bank of counters in the digital electronics. The maximum count rate for each sector is limited by the deadtime (τ), which is effectively the time it takes the electronics to process a single event. During this time the detector is insensitive to any additional events, so the integration time is reduced by the factor $(1 - R'\tau)$, where R' is the measured count rate. The true count rate (R) is then:

$$R = R'(1 - R'\tau)^{-1}$$

The deadtime of the MCP-anode-preamp chain was measured to be 2.8×10^{-6} sec. The maximum true count rate per sector that can be reliably corrected for deadtime using the equation above is ~10^6 s^{-1}. Data are flagged as bad whenever $R' > 0.8/\tau$.

The field of view of the concentric hemispheres alone (with no voltage applied to the deflectors) is 360° x 7° (azimuth × elevation). An energy spectrum is obtained by sweeping the inner hemisphere potential from 0.5 to 750 V. With a measured analyzer constant of $K_a = 6.17$, this corresponds to an energy range of 3 to 4600 eV. The energy resolution is set by the gap between the hemispheres, and was measured to be ΔE/E (FWHM) = 17%.

Electrons entering the aperture pass through two concentric toroidal grids. The outer grid is tied to chassis ground (which is in turn tied to spacecraft ground), while the voltage of the inner grid can be commanded between 0 and −25 V. The electrical design is such that all surfaces interior to the inner toroidal grid (hemispheres, deflectors, top cap, exit grid) are referenced to the potential of the inner grid. In this way, the toroidal grids act as an electrostatic attenuator, decelerating incoming electrons without altering their trajectories or the electrostatic optics interior to the grids. This bias voltage, V_0, is controlled by the instrument's sweep table. One mode of operation scales V_0 to the analyzer voltage:

$$V_0 = \frac{E''}{2} = \frac{V_A K_a}{2}$$

where E" is the energy of electrons *after* they have been decelerated through the toroidal grids, and V_A is the potential difference between the inner and outer hemispheres. In this way, the energy resolution (ΔE/E) is reduced by the factor $f = 1/(1 + V_0/V_A K_a) = 2/3$, and the geometric factor is reduced by f^2. This mode is effective up to energies of E" = 50 eV (since the maximum value of V_0 is −25 V), or E' = 75 eV just outside the outer grid. The mode can be disabled simply by setting V_0 to zero throughout the sweep.

Electron angular distributions typically span the full sky, so it is important that the field of view (FOV) be as large as possible. On a spinning spacecraft, the instrument symmetry axis can be oriented orthogonal to the spin axis, which would sweep the hemispheres' 360° x 7° FOV over the full sky every half-spin. However, MAVEN is a three-axis stabilized spacecraft, so SWEA uses deflectors to sweep the field of view in elevation by ±60°, resulting in an overall FOV of 360° × 120°, which represents 87% of the sky. The instrument is located at the end of a 1.5-meter boom (Fig. 2), at which distance the spacecraft blocks 8% of SWEA's FOV. The unobstructed FOV is thus 79% of the sky.

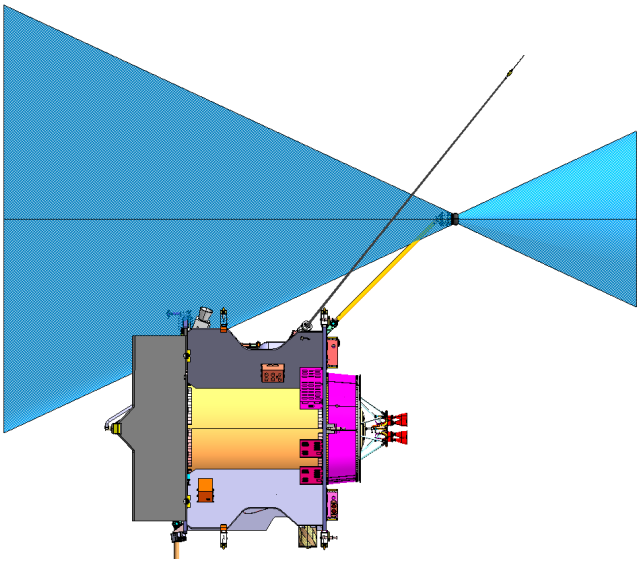

Figure 2: SWEA is on the end of a 1.5-meter boom, with a 360° × 120° field of view. (Blue shading indicates SWEA's blind spots.) The instrument's symmetry axis is parallel to the high gain antenna axis (spacecraft Z). When the spacecraft Z axis points to the Sun, the SWEA electronics box shields the analyzer (including the toroidal entrance grids) from sunlight. This eliminates photoelectron production from the toroidal grids and within the aperture.

The deflection angle is a linear function of the ratio of the deflector voltage (V_D) to the analyzer voltage (V_A):

$$\theta\ [deg] = 10.89\left(\frac{V_D}{V_A}\right) - 0.90$$

Thus, the deflection voltage needed to achieve a given deflection angle is proportional to the analyzer voltage (See section 2.6.2). The use of deflectors results in a non-uniform angular resolution in elevation. This is a property of the electrostatic optics, and results from the fact that the electrons can be deflected in the same or opposite sense as the trajectory within the hemispheres. The elevation resolution is 7° (FWHM) when the deflectors are both at ground (0° elevation), reaches a minimum of 3.3° at +30° elevation, and varies from about 15° at −60° elevation to 10° at +60° elevation. A more uniform elevation resolution is obtained by averaging over discrete deflector settings, so that the effective resolution is similar to the 22.5° azimuth resolution.

The geometric factor is a combination of electrostatic optics, grid transmissions, and MCP efficiency. The geometric factor was measured at IRAP using a calibrated electron beam and found to be G = 0.009 cm^2 ster eV/eV for all 16 anodes. The maximum energy flux that can be reliably measured is the maximum count rate per sector divided by the geometric factor per sector:

$$F_{max} = \frac{10^6\ s^{-1}}{5.6 \times 10^{-4}\ cm^2\ ster} = 1.8 \times 10^9\ eV\ cm^{-2}\ s^{-1}\ ster^{-1}\ eV^{-1}$$

2.1 Science Objectives

SWEA measures the energy and angular distributions of 3- to 4600-eV solar wind and magnetosheath electrons and ionospheric photoelectrons. With these measurements, the instrument: (1) determines the electron impact ionization rates in all regions sampled by MAVEN, (2) distinguishes the energy spectra of ionospheric primary photoelectrons and of solar wind, magnetosheath, and magnetotail electrons to determine plasma environment, (3) calculates electron pitch angle distributions to determine the topology of magnetic fields from both external and crustal sources, and (4) identifies auroral (~keV) electron populations and determines their role in ionization and dissociation processes.

2.2 Instrument Operation

SWEA has a 2-second measurement cycle. The instrument takes data over the first 1.95 sec, as the potential difference between the hemispheres sweeps from its highest value of 750 V down to 0.5 V. This is followed by a 0.05-sec "gap", during which time the instrument does not take data as the analyzer potential ramps back up and settles at 750 V in preparation for the next measurement cycle. The 1.95-sec data collection interval is divided into 1792 equal steps. During each of these steps, the analyzer and deflector voltages (V_A,V_{D1}, and V_{D2}) and V_0 are commanded to discrete values according to the sweep pattern shown in Fig. 3. The analyzer voltage is commanded to 64 logarithmically spaced values from 750 V to 0.5 V, for a duration of 28 steps each. During each analyzer voltage setting, the deflectors are swept in linear ramps that are proportional to the analyzer voltage. This provides a constant angular coverage and resolution as a function of energy until the deflectors reach their maximum potential. To achieve a maximum deflection of 60°, the ratio V_D/V_A must be 5.5. Thus, for a maximum deflector potential of 1800 V (limited by the high voltage power supply), full deflection is achieved up to an analyzer voltage of 327 V, corresponding to an electron energy of 2 keV. At higher energies, the maximum deflection angle is inversely proportional to energy, falling to 26° at 4.6 keV.

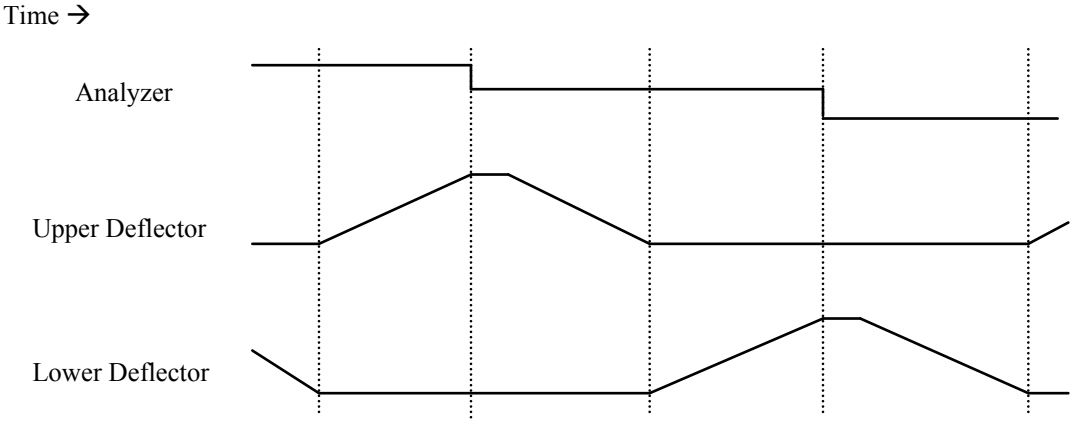

Figure 3: Sweep pattern for the analyzer and deflector voltages. When enabled, V0 (not shown) is scaled to the analyzer voltage up to a maximum value of −25 V. Vertical dotted lines are at ~15 millisec intervals. Voltages are not to scale.

During the first 4 steps of each analyzer setting, the deflector voltages remain constant to allow time for all voltages to settle. (Data collected during these first 4 steps are later discarded by the PFDPU.) During the next 24 steps, the upper and lower deflectors are alternately ramped, while data are accumulated for each of the 16 anodes in 4-step intervals. This provides six elevation bins with ~20-degree elevation resolution (up to 2 keV), which is similar to the 22.5-degree azimuth resolution and partially compensates for the instrument's intrinsic variable elevation resolution. Above 2 keV, the deflection bin sizes scale with the maximum deflection angle, providing uniform deflection angle coverage as the FOV shrinks. There are a total of 16×6 = 96 azimuth-elevation bins for each of 64 energy bins.

2.3 Measured Parameters

During each 2-second measurement cycle, SWEA generates 448 messages (4-step accumulations of the 1792 data collection steps), with each message consisting of sixteen 16-bit counter values, one for each anode. The accumulation time per anode is 1.95/448 = 4.35 msec. The PFDPU discards the first of every seven messages that comprise the deflector sweep (to allow for setting time) and organizes the remaining 384 messages into a 64-energy × 16-azimuth × 6-elevation distribution. In order to make best use of SWEA's total telemetry allocation, the PFDPU calculates three data products from this distribution: 3D spectra, pitch angle distributions (PADs), and energy spectra (SPECs). The cadence of each data product is a multiple of 2 sec, which can be set independently of the other data products. All three data products are synchronized, so that each 3D product corresponds precisely to PAD and SPEC data products obtained over the same measurement cycle. This makes it possible to intercompare the data products, which are summed on-board in different ways and sampled with different cadences.

As it receives SWEA data messages, the PFDPU sorts the data in energy and angle, accumulating counts in 19-bit registers. At the end each accumulation interval, the 19-bit values are compressed to 8 bits using a scheme that provides 1-count resolution up to 32 counts, 2-count resolution for the next 16 values, 4-count resolution for the next 16, and so on (Table 5).

Table 5: 19-to-8 Compression

0	1	2	3	4	5	6	7	8	9	10	11	12	13	14	15
16	17	18	19	20	21	22	23	24	25	26	27	28	29	30	31
32	34	36	38	40	42	44	46	48	50	52	54	56	58	60	62
64	68	72	76	80	84	88	92	96	100	104	108	112	116	120	124
128	136	144	152	160	168	176	184	192	200	208	216	224	232	240	248
256	272	288	304	320	336	352	368	384	400	416	432	448	464	480	496
512	544	576	608	640	672	704	736	768	800	832	864	896	928	960	992
1024	1088	1152	1216	1280	1344	1408	1472	1536	1600	1664	1728	1792	1856	1920	1984
2048	2176	2304	2432	2560	2688	2816	2944	3072	3200	3328	3456	3584	3712	3840	3968
4096	4352	4608	4864	5120	5376	5632	5888	6144	6400	6656	6912	7168	7424	7680	7936
8192	8704	9216	9728	10240	10752	11264	11776	12288	12800	13312	13824	14336	14848	15360	15872
16384	17408	18432	19456	20480	21504	22528	23552	24576	25600	26624	27648	28672	29696	30720	31744
32768	34816	36864	38912	40960	43008	45056	47104	49152	51200	53248	55296	57344	59392	61440	63488
65536	69632	73728	77824	81920	86016	90112	94208	98304	102400	106496	110592	114688	118784	122880	126976
131072	139264	147456	155648	163840	172032	180224	188416	196608	204800	212992	221184	229376	237568	245760	253952
262144	278528	294912	311296	327680	344064	360448	376832	393216	409600	425984	442368	458752	475136	491520	507904

Raw 19-bit values are rounded down, so each 8-bit value corresponds to a range of possible counts. For example, a telemetry value of 96 decompresses to 512, which corresponds to a range of 512-543 counts. The middle of each range is provided in the SWEA data products, so it is possible to have half counts. The maximum number of counts in this scheme is 524287 ($2^{19} - 1$), which is rounded down to 507904. This 2.5 times larger than needed, even when the instrument

is counting at its maximum rate. Since each telemetry value corresponds to a range of possible counts, this scheme introduces digitization noise, which dominates the statistical variance at high count rates.

If we approximate digitization noise as additive white noise, then the variance, *S*, is given by:

$$S = N + \frac{(M^2 - 1)}{12}$$

where *N* is the decompressed counter value, and *M* is the total number of 19-bit values that map into *N*. Using the example above: $N = 527.5$, $M = 32$, and $S = 612.75$. Note that at 1-count resolution ($M = 1$), there is no contribution from digitization noise.

2.3.1 3D Distributions

At the highest resolution, a 3D spectrum consists of 64 energies × 16 azimuths (anode bins) × 6 elevations (deflection bins). Adjacent azimuth sectors are averaged at the highest positive and negative elevations to provide a more uniform solid angle resolution. For ease of use, we maintain 16 azimuth bins for all elevations. For the highest positive and negative deflections, we duplicate the binned counts for each pair of binned azimuths and maintain an angular binning factor for subsequently calculating count rate or converting to physical units. (Duplicating the counts in two adjacent bins effectively doubles the integration time for each of those bins.) The angular binning factor is 2 for the highest positive and negative deflections, and 1 for all other deflections. The distribution can be further averaged in groups of 2 or 4 adjacent energy steps. We duplicate binned counts in groups of 2 or 4, as appropriate, to maintain 64 energy bins. This introduces an energy binning factor, which is used in the same way as the angular binning factor. Finally, the distribution can be sampled every 2^N two-second measurement cycles, where N is an integer ($N \geq 0$). Raw decompressed counts and binning factors are provided in the 3D data products to allow calculation of statistical uncertainties; however, care must be taken, since duplicated bins are not independent.

2.3.2 Pitch Angle Distributions

The most scientifically relevant way to organize the electron angular distribution is with respect to the magnetic field. The angle between an electron's velocity vector and the magnetic field vector is defined as the "pitch angle", which ranges from 0° (parallel) to 180° (anti-parallel). These pitch angle distributions (PADs) are generated onboard by flight software in the PFDPU. The first step is to perform a basic calibration of the magnetic field vector and then rotate the vector into SWEA instrument coordinates, so that the 96 azimuth-elevation pairs can be mapped into pitch angle. The pitch angle distribution that is placed in telemetry is composed of 16 values: one for each of the 16 azimuth sectors. Flight software determines the optimal deflection bin for each azimuth sector that maximizes the total pitch angle coverage. The solution is a great circle entirely within the FOV that contains the magnetic field vector, or comes as close a possible to doing so. This guarantees that a complete pitch angle distribution is obtained whenever the magnetic field vector is within SWEA's FOV, and that any gaps are not larger that the instrument's intrinsic blind spots ($|\theta| > 60°$, see Figure 2).

Since the 16 PAD bins span 360° in azimuth, there is two-fold redundancy. That is, the pitch angle distribution is measured twice, once for each half of the detector. This redundancy can be

used to monitor the calibration in fight, which is expected to change gradually as the MCPs age. The basic calibration performed onboard is sufficient to optimize the pitch angle coverage provided by this data product. No information is lost in producing a PAD onboard, since it is obtained without averaging in angle. To produce calibrated L2 PAD data, the pitch angle mapping is refined on the ground by using fully calibrated Magnetometer data. The average pitch angle and the range of pitch angles spanned by each bin is provided in the PAD data product.

PADs can be averaged in groups of 2 or 4 adjacent energy steps. As before, we duplicate binned counts, as appropriate, to maintain 64 energy bins. The distribution can also be sampled every 2^N two-second measurement cycles. The PAD energy binning and time sampling can be different from those used in the 3D data product. Raw decompressed counts and binning factors are provided in the PAD data products to allow calculation of statistical uncertainties.

2.3.3 Energy Spectra

Energy spectra are obtained by taking a weighted average of all 96 azimuth-elevation bins. Before summing, the counts are multiplied by cos(θ) to account for variation of the solid angle spanned by each bin:

$$\Delta\Omega = 2\,\Delta\phi\,\sin\left(\frac{\Delta\theta}{2}\right)\cos\theta$$

where Δϕ and Δθ are the angular widths in azimuth (22.5°) and elevation (20°), and θ is the center elevation. To within a constant scaling factor, this weighted summation over angular bins approximates the angular summation of a density moment calculation. The energy summation can be performed on the ground, or the energy spectrum can be fit with a model to estimate density and temperature.

A weighting factor is provided in the SPEC data product to allow conversion of weighted counts to mean raw count rate per anode, which allows an estimate of dead time for the summed data. The 3D data can be used to evaluate the accuracy of this estimate, albeit at a lower cadence. Energy spectra always contain all 64 energy steps to provide the best possible energy resolution, and they can be either sampled or summed over every 2^N two-second measurement cycles.

2.4 Operational Modes

The instrument has one operational mode, which produces 448 messages synchronized to the sweep pattern every 2-second measurement cycle. Energy averaging and time sampling are performed in the PFDPU when calculating the three SWEA data products. Energy sampling for 3D and PAD products and time sampling for all three products are parameterized and can be adjusted by command to manage SWEA's data production rate. Thus, as the overall telemetry bandwidth varies during the mission (because of the changing Earth-Mars distance), SWEA's data production can vary accordingly.

The energy and time sampling parameters are used to define two data collection modes: solar wind mode and ionosphere mode. Solar wind mode is used at high altitudes, where high resolution is less important. This allows us to expend a greater fraction of SWEA's total telemetry allocation to achieve higher resolution at low altitudes. The transition altitude between

these two modes is adjustable on the ground; it will be 2000 km at the start of science operations in November 2014.

Each data collection mode produces two data streams: survey and archive. The survey stream provides sufficient resolution to achieve SWEA's scientific goals, and is placed into telemetry in its entirety. The archive stream contains higher energy and/or time resolution and is stored in flash memory within the PFDPU. Only a fraction of the archive data can be telemetered to the ground. Telemetry bandwidth for sending archive data is obtained by lossless compression of the survey data stream. Typically a factor of ~2 compression is achieved, which provides space for ~10% of the archive data. At each contact (nominally twice per week), survey data are reviewed and time ranges of interest are selected. Commands are then sent to the PFDPU at the next contact to downlink the archive data covering the desired time range(s). The archive data have the same format as the survey data. The only differences are the energy and/or time resolutions.

Each of the data products is a time series of an array with dimensions of energy and angle. Changes in time sampling are naturally accounted for in the time series. The number of angles is fixed for each product: 3D (96), PAD (16), and energy spectra (no angle dimension). As noted above, Energy spectra always have 64 energy channels. However, changes in energy averaging can alter the dimensions of the energy/angle arrays. To maintain fixed array dimensions for each of the data products (3D, PAD, energy spectra), all arrays are sized to accommodate the maximum number of energy channels (64). When energy averaging reduces the number of energy bins to 32 or 16, the raw counts are duplicated in groups of 2 or 4 adjacent energy bins to maintain a total of 64 bins, and a binning factor (B = 2 or 4) is recorded to allow calculation of raw count rate.

2.5 Operational Considerations

2.5.1 Spacecraft Charging and Photoelectrons

A spacecraft orbiting Mars can experience widely different environments in terms of plasma density, electron temperature, and ionizing radiation. Solar ultraviolet light causes photoelectron emission, which represents a positive current into the spacecraft. Impacts of ambient charged particles also represent a current to the spacecraft, with the net plasma current negative because electrons have higher thermal velocities (and therefore fluxes) than do ions. Other currents are produced by secondary emission of electrons generated by electron and ion impact, but these currents are highly material-dependent. The spacecraft responds almost instantly to these different environments by reaching an electrostatic potential such that the net current to the spacecraft is zero. This potential affects plasma measurements by shifting the energies of incoming ions and electrons, bending the trajectories of low energy and low mass charged particles, and repelling like-charged particles with energies at or below the potential.

In low density environments (basically anywhere outside the ionosphere) when the spacecraft is in sunlight, the dominant current results from photoelectrons emitted by the spacecraft. This causes the spacecraft to charge positive until it reaches a potential sufficient to attract enough photoelectrons back to the spacecraft to achieve zero net current. The magnitude of this potential depends on the flux of ionizing radiation and the local plasma density, as well as the photoemission and secondary emission properties of the spacecraft. Typical values upstream of

Mars' bow shock and in the magnetosheath, where the ambient density exceeds a few × 10^{-1} cm^{-3}, range from a few volts up to +10 V.

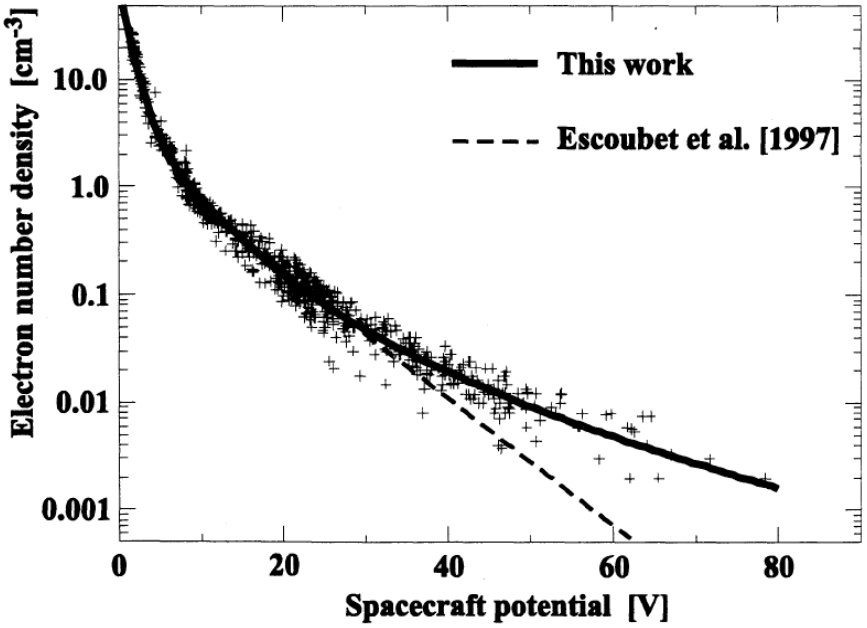

Figure 4: Charging of the Geotail spacecraft in sunlight. (Ishisaka et al., 2001). The curve for MAVEN has not yet been measured but is expected to be similar.

By tracking the positions of low-energy features in the electron energy spectrum, the ASPERA-3-ELS experiment onboard Mars Express measured spacecraft potentials in the magnetosheath of typically less than +8 V, although potentials up to +10 V were occasionally observed (Frahm *et al.* 2006).

In the ionosphere, where the plasma density is orders of magnitude higher (Figure 5), the current resulting from ambient charged particles impacting the spacecraft can dominate the photoelectron current, and the spacecraft will charge to a negative potential comparable in magnitude to the local electron temperature. Below ~200 km altitude, the ionospheric electron temperature is a few hundredths of an eV, increasing to a few tenths of an eV from ~200 to ~400 km. When in the ionosphere, the ELS instrument on Mars Express measured potentials of a few volts negative (Frahm *et al.* 2006).

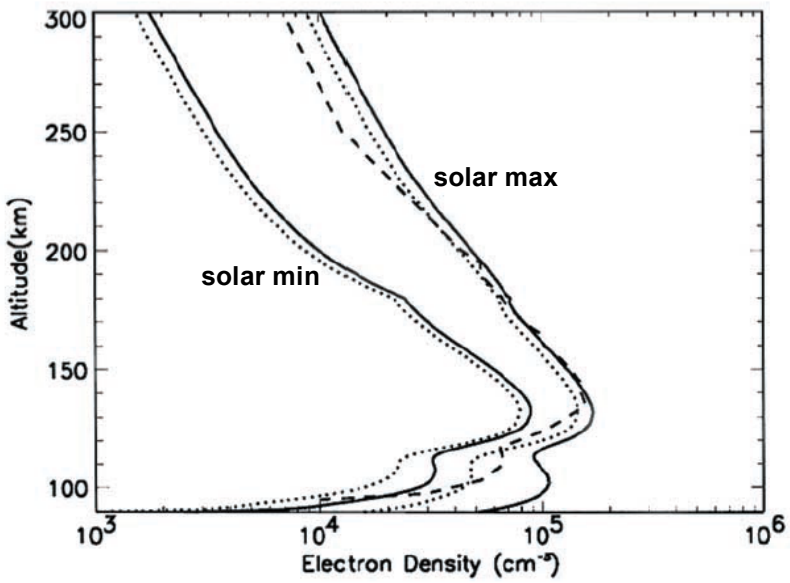

Figure 5: Electron density profiles in Mars' ionosphere away from crustal magnetospheres for solar minimum and maximum conditions (after Fox 2004).

The largest potentials should occur when the spacecraft is in the magnetotail and in the planet's shadow, where photoemission is absent. The relatively high electron temperatures in this region typically result in spacecraft potentials of several tens of volts negative, as estimated from MGS Electron Reflectometer data by comparing electron energy spectra obtained in the optical shadow with those obtained in sunlight. Much larger negative potentials (hundreds to thousands of volts) have been observed in shadow in the Earth's magnetosphere (cf. Whipple, 1981 and references therein) when energetic electron populations are present. Such large potentials could also occur at Mars.

At high altitudes in sunlight, MAVEN charges to a positive potential (ϕ) of several volts. Spacecraft photoelectrons with energies below ϕ are attracted back to the spacecraft, while those with energies above ϕ escape. Meanwhile, ambient electrons are attracted to the spacecraft and shifted in energy. Thus, an instrument mounted on (and at the same potential as) the spacecraft measures spacecraft photoelectrons below ϕ and ambient electrons above ϕ. SWEA's energy range extends down to 3 eV, so that both populations are typically observed. The boundary between the two populations is marked by a sharp change or reversal of slope in the energy spectrum at $E = \phi$. Energy spectra, with 64 energy channels, can be used to provide the most accurate measure of ϕ, which can then be used to correct the energy scales of all three data products. An independent measure of the spacecraft potential is provided by the Langmuir Probe and Waves (LPW) experiment. LPW can provide estimates of spacecraft potential outside of SWEA's range ($\phi > +3$ V).

2.5.2 Field of View and Spacecraft Blockage

If there were no spacecraft, SWEA's 360° × 120° field of view (FOV) would cover 87% of the sky. However, even on the end of a boom, 8% of the sky within SWEA's FOV is blocked by the spacecraft. SWEA is at a fixed location at the end of a 1.5-meter boom (Fig. 2), so the spacecraft maps into a fixed range of azimuth and elevation. The affected angular bins are flagged in the 3D and PAD data products.

2.5.3 Energy-Dependent Field of View

As described in Section 2.2, SWEA's field of view is energy dependent above 2 keV, because the deflector high voltage supply tops out at 1800 V. Above 2 keV, the deflection range decreases with energy, ranging from ±60° (full deflection) at 2 keV to ±26° at 4.6 keV. The elevation bins are scaled accordingly to provide uniform angular sampling within the available range. Since the FOV depends on the sweep pattern (Fig. 3), it is possible for the FOV to change during the mission if the sweep pattern changes. Consequently, an energy-azimuth-elevation array is provided to describe SWEA's energy-dependent field of view.

Note that pitch angle distributions are more likely to have reduced coverage as the instrument's FOV shrinks at energies above 2 keV. The algorithm for optimizing the pitch angle coverage of the PAD data product was designed for the full ±60° deflection range, and will be less effective for reduced deflection ranges.

2.6 Ground Calibration

2.6.1 Energy-Angle Response

The instrument energy-angle response was measured in a calibration vacuum chamber for manipulator yaw values ranging from −50° to +60°. (Contact between the harness and the chamber wall prevented more negative yaws.) With the electron beam energy held constant at 1 keV, the analyzer and deflector voltages were varied to map the response function.

In the following figures, the measured response is compared with simulations for three sample yaws: 0° and ±45°. Energy is represented as K, which is the ratio of the electron beam energy to the potential difference between the hemispheres (V_A). Deflection angle is a linear function of the ratio of the deflector potential to the analyzer potential (V_D/V_A). This function is calibrated and used to convert V_D/V_A to angle in the measured distributions. In the simulations, angle is determined directly from the particle trajectories.

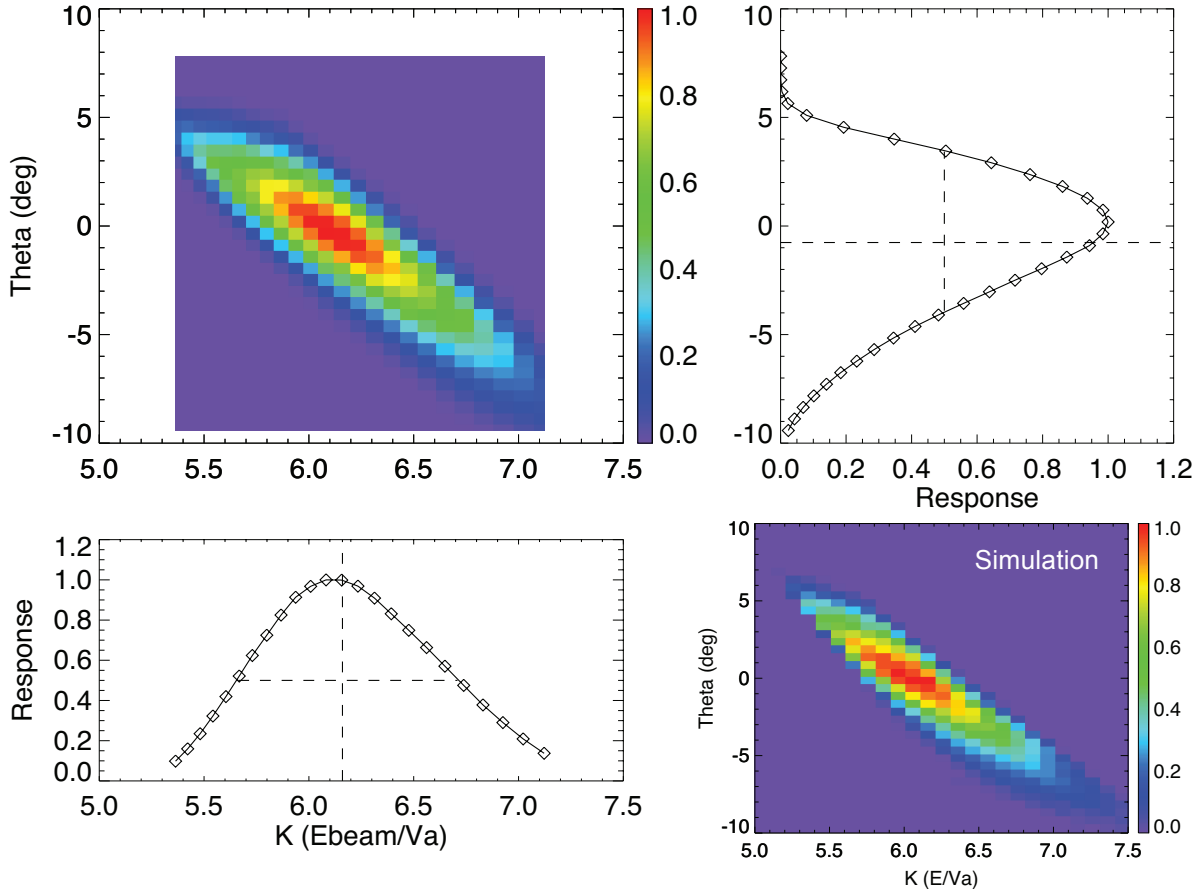

Figure 6: Measured energy-angle response, normalized to unity, at a mechanical yaw of 0 deg (top left). Theta is the deflection angle achieved by varying the deflector voltages (see Fig. 9), and K is ratio of the beam energy (Ebeam) to the analyzer voltage (Va). In this calibration run, the beam energy was held constant while the analyzer voltage was varied. The line drawings are the integrated responses, renormalized to unity, in angle (upper right) and energy (lower left). The simulation (lower right) has been shifted by ΔK = −0.44 (see text).

The simulated response must be shifted by ΔK = −0.44 to provide the best agreement with the measured response. This corresponds to a slight increase (~0.2 mm) in the actual gap between the hemispheres compared with the simulated geometry. This difference can be attributed to two sources. First, the simulated geometry does not include scalloping of the inner and outer hemispheres and the top cap. These rounded grooves are 0.24 mm in depth relative to the simulated radii of curvature, so the effective gap is expected to be larger than the simulated gap. Second, the observed variation in K as a function of azimuth (see below), which is a measure of hemisphere concentricity, indicates that mechanical tolerances are of order 0.1 mm. After shifting the simulated energy-angle response, the agreement between measurement and simulation is excellent.

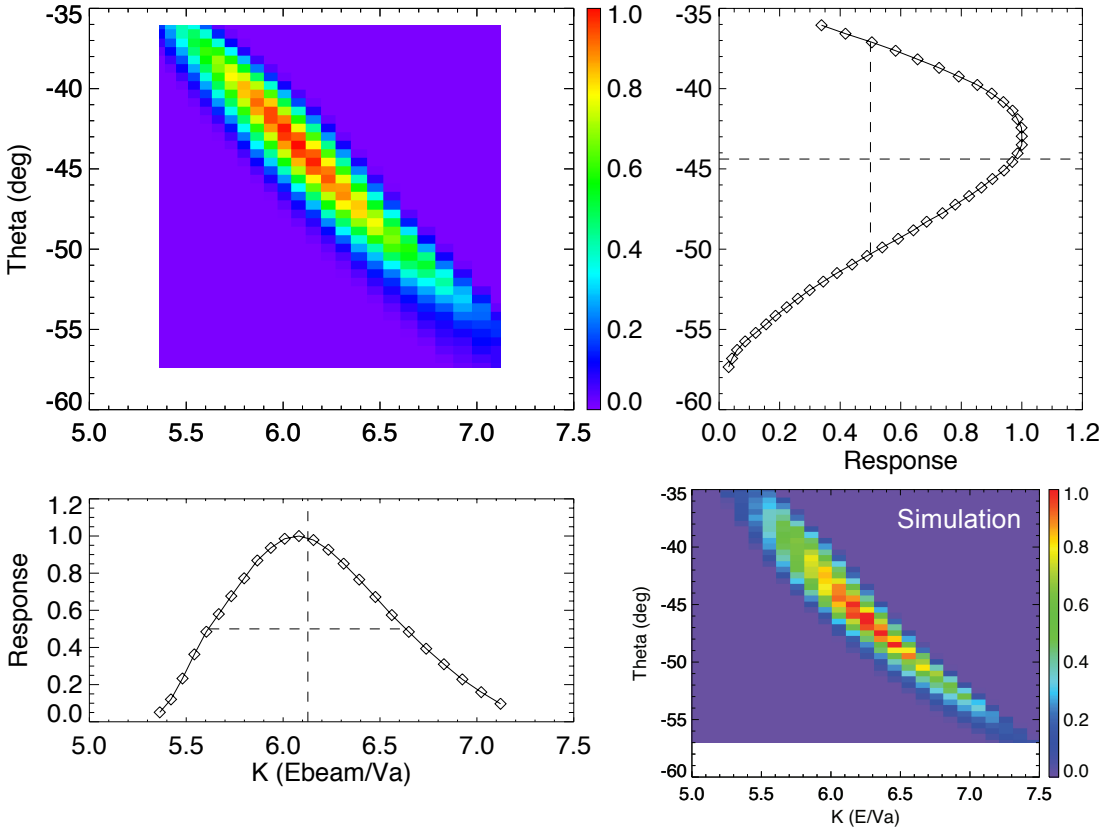

Figure 7: Measured energy-angle response (top left and both line drawings) and simulated response (lower right) for a yaw of −45°. In the simulation, K is shifted by the same amount as for zero yaw. See caption to Fig. 6.

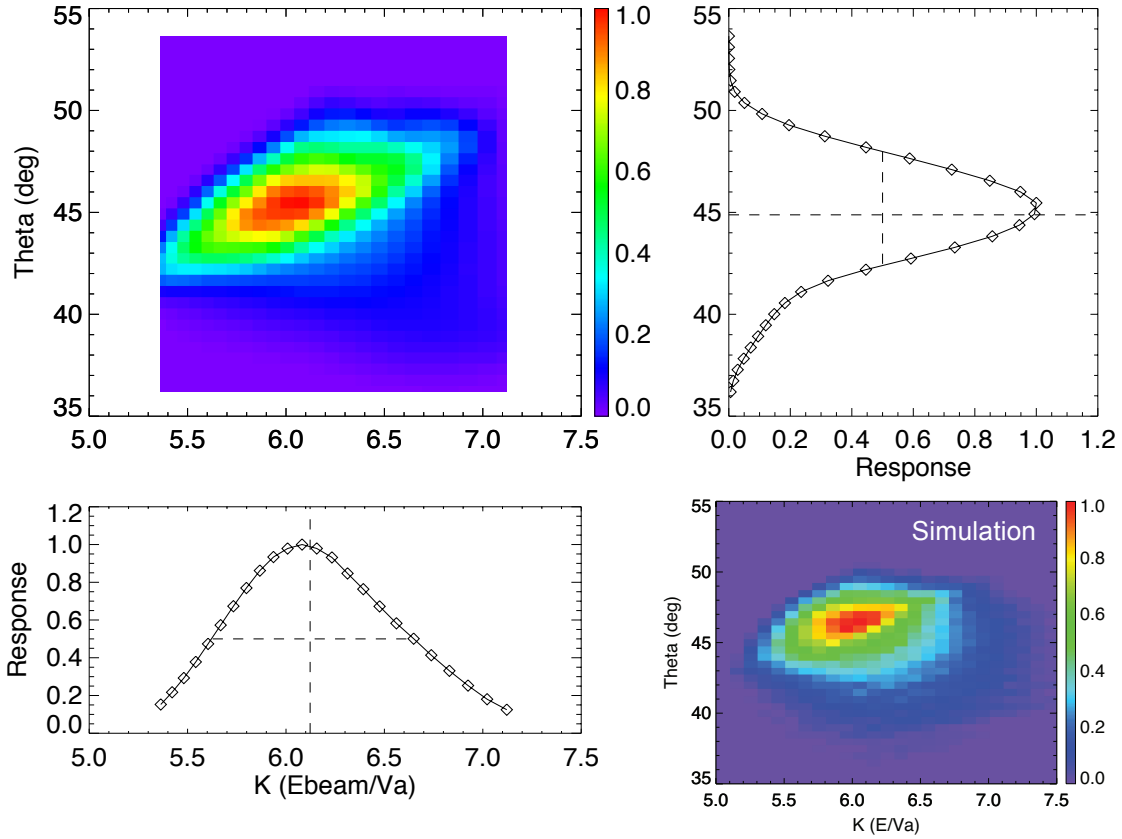

Figure 8: Measured energy-angle response (top left and both line drawings) and simulated response (lower right) for a yaw of +45°. In the simulation, K is shifted by the same amount as for zero yaw. See caption to Fig. 6.

2.6.2 Deflector Calibration

Measured response functions at manipulator yaws ranging from −50° to +60° were used to determine the relationship between deflection angle and the ratio of the deflector potential (V_D) to the analyzer potential (V_A). Simulations predict that this relationship should be very nearly linear over the full deflection range, until the deflectors themselves begin to impinge on the FOV at the largest deflection angles.

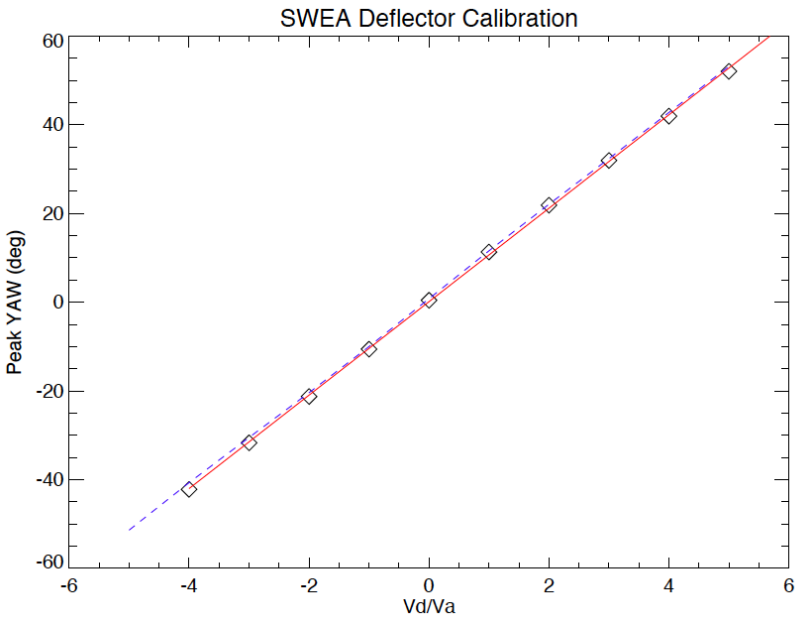

Figure 9: Mechanical yaw as a function of V_D/V_A. Diamond symbols are the measured values, and the red line is a linear fit to those measurements. The blue dashed line is derived from detector simulations.

The measurements (upward and downward deflections combined) are well fit with a linear function:

$$\theta\,[deg] = 10.89\left(\frac{V_D}{V_A}\right) - 0.90$$

This agrees with simulation to within ~1°, which is comparable to the accuracy with which the instrument is mounted to the manipulator, and is much smaller than the instrument's elevation resolution (~20 deg).

2.6.3 Analyzer Constant and Energy Resolution

The analyzer constant (K_a) is the ratio of the energy of transmitted electrons to the potential difference between the hemispheres (or analyzer voltage, V_A). The beam energy is held constant while the analyzer energy-angle response is measured, as described above. Integrating this distribution over angle provides an energy response function (Fig. 10). The weighted mean value of K for this distribution (Σ (K×R) / Σ R), where R is the normalized response) is the analyzer constant, and the full width at half maximum (FWHM) is a measure of the energy resolution.

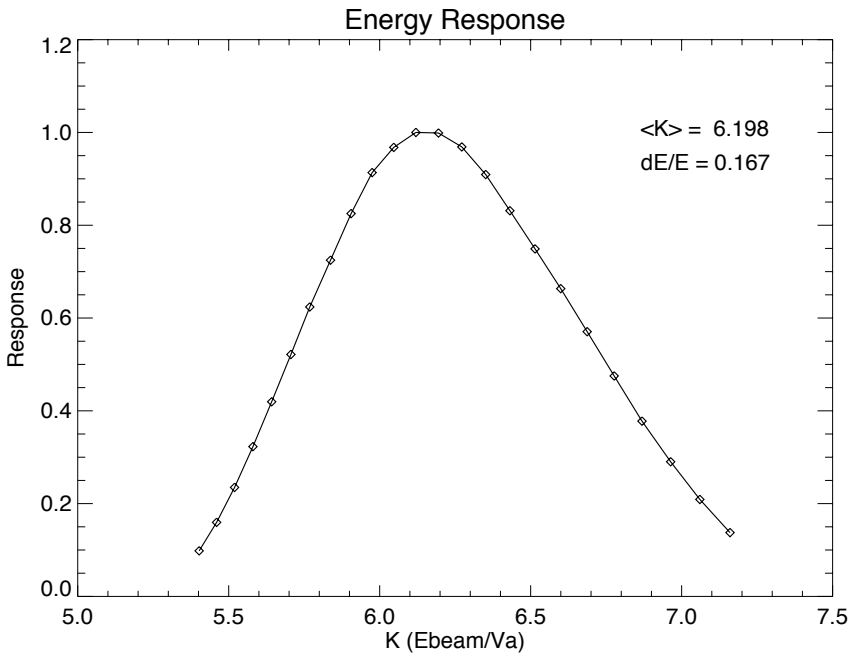

Figure 10: Energy response obtained by integrating the measured energy-angle response function at a yaw of zero (Figure 6). The weighted mean value of K and the energy width (ΔE/E, FWHM) are indicated.

The analyzer constant measurement was repeated as a function of azimuth (Fig. 11) by setting manipulator roll to 16 positions around the 360° FOV, all with yaw at 0.

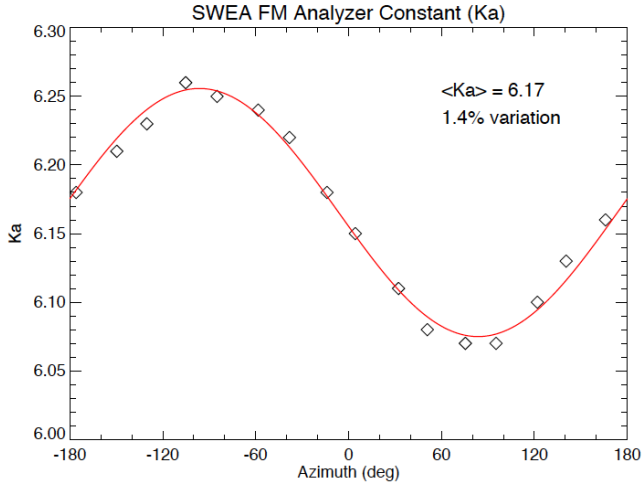

Figure 11: Analyzer constant (K_a) as a function of azimuth around the FOV. The red line is the best fit sine function.

The results are well fit with a sine function, which indicates that the most likely cause for the variation in a slight misalignment of the hemispheres. A misalignment of ~0.1 mm would explain the amplitude of the variation. This results in a 1.4% variation in the energy response around the field of view, which is small compared with the energy resolution (ΔE/E, FWHM) of 17%.

The analyzer constant and energy resolution do not vary significantly with elevation up to +55°. (The experimental setup at SSL did not permit yaws less then −50°.) Table 6 summarizes results as a function of yaw. The value for yaw = 0 corresponds to Figures 6 and 10.

Table 6: Analyzer constant and energy resolution as a function of mechanical yaw with respect to the beam direction.

YAW	<K>	ΔE/E (FWHM)
−45	6.166	0.160
−30	6.188	0.169
0	6.198	0.167
+30	6.164	0.167
+45	6.161	0.169
+55	6.156	0.168

2.6.4 Azimuthal Response and Field of View

The azimuthal response of the instrument was measured by setting the instrument voltages for the center of the response function for a 4 keV beam at yaw = 0 and then rotating the detector at a constant rate about the symmetry axis by 380° (to provide some overlap). As the instrument rotates and collects data, each anode in turn is illuminated by the electron beam.

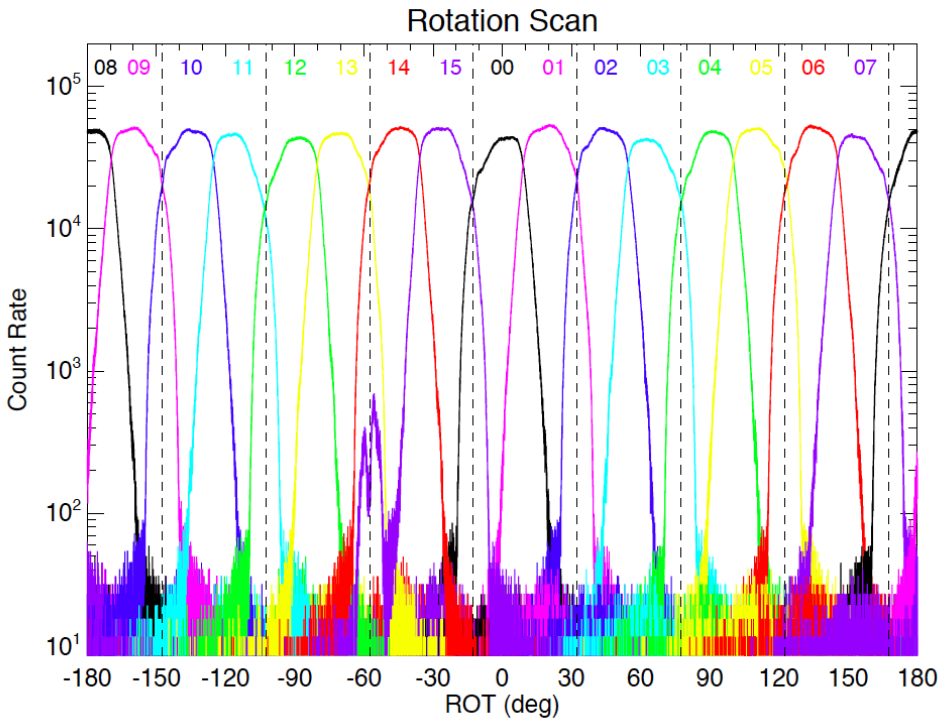

Figure 12: Detector response as a function of azimuth around the field of view at yaw=0. The responses of all 16 anodes (numbered 0 through 15) are shown. Vertical dashed lines indicate the locations of support ribs for the toroidal grids.

The 16 sectors provide 22.5° resolution over a 360° range of azimuth. There is no measureable cross talk between the sectors, except for sector 15, which exhibits peak cross talk at the ~1% level.

2.7 In-flight Calibration

Angular and energy resolution and accuracy is determined for SWEA, SWIA, and STATIC by calibration on the ground and verification of electrostatic optics simulations. Therefore, the only unknown is the absolute sensitivity of the instrument, which depends on the absolute efficiency of the microchannel plates (MCPs). Therefore, it suffices to use the total plasma density measured by each analyzer as a calibration point to determine the absolute MCP efficiency.

LPW measures the plasma frequency between 90 kHz and 1.67 MHz, which corresponds to a total plasma density between 100 cm^{-3} and 3×10^4 cm^{-3}. This density range will be seen throughout the upper ionosphere, allowing many measurements of plasma density that can be compared with STATIC. LPW measurements of plasma frequency are sufficient to determine the plasma density to within 5%.

In the ionosphere, STATIC will measure ram ions. Since the ram velocity of the spacecraft is much larger than the local thermal velocity and the ram energy of the ions is much larger than the expected spacecraft potential, STATIC will measure the entire ion distribution. Therefore,

the only limiting factors on the accuracy of the ion density measurement from STATIC in the upper ionosphere are the spacecraft potential, and Poisson counting statistics.

For a typical periapsis velocity of ~4.5 km/s and an ion mass in the 16-32 range, the ram energy of the ions is on the order of 2 eV. Meanwhile, the plasma temperature and the spacecraft potential will be on the order of 0.1 eV in the ionosphere. For these values, even if we had no a priori knowledge of the spacecraft potential, STATIC could provide density measurements with a relative accuracy of ~0.1/2.0 = 5% (STATIC essentially measures the flux, n×v, so the error in v resulting from the spacecraft potential can be directly related to an error of the same magnitude in n).

In fact, we should also have some a priori knowledge of the spacecraft potential both from the shape of the measured distribution functions and from the I-V curve measured by LP, which will increase the fidelity of this measurement still further.

Finally, count rates are large enough that errors from Poisson statistics should be essentially negligible, certainly less than 5%.

Therefore, even in the worst case of error propagation, we expect to be able to calibrate STATIC plasma density measurements in the ionosphere to better than 15%. In fact, errors should add in quadrature, so we can calibrate STATIC to 10%.

As an alternative, STATIC can determine absolute START and STOP efficiencies from ratios START/(START+STOP) and STOP/(START+STOP) events, which can be combined with mechanical analyzer geometric factor knowledge from electrostatic optics simulations to get an absolute sensitivity, with error determined by mechanical tolerance and supported by analyzer energy constant. This procedure will work whenever one ion species dominates – for instance in the solar wind or outer magnetosheath. The results of this analysis should agree with cross calibration with LPW, providing a consistency check.

SWIA and STATIC can be calibrated directly to each other in the magnetosheath or in the solar wind at times with less intense fluxes. This calibration can be performed without any requirement for measuring or calculating a total density, since the two sensors have overlap in both energy and angular coverage. Since the two sensors have exactly the same analyzer electrostatic optics, there are very few uncertainties in this calibration. We estimate that this calibration can easily be made to an accuracy of 5%. Therefore, SWIA can be calibrated to better than 15% (assuming 10% accuracy of STATIC calibrations).

Finally, SWEA can be calibrated to both SWIA and STATIC in the sheath and/or solar wind. This is a well-understood procedure with extensive heritage from THEMIS and other spacecraft. We estimate that this calibration can easily be done to 10% accuracy, ensuring that SWEA can be calibrated to better than 25%.

3 Data Overview

This section provides a high level description of archive organization under the PDS4 Information Model (IM) as well as the flow of the data from the spacecraft through delivery to PDS. Unless specified elsewhere in this document, the MAVEN SWEA archive conforms with version 1.1.0.1 of the PDS4 IM [4] and version 1.0 of the MAVEN mission schema. A list of the XML Schema and Schematron documents associated with this archive are provided in Table 7 below.

Table 7: MAVEN SWEA Archive Schema and Schematron

XML Document	Steward	Product LID
PDS Master Schema, v. 1.1.0.1	PDS	urn:nasa:pds:system_bundle:xml_schema:pds-xml_schema
PDS Master Schematron, v. 1.1.0.1	PDS	urn:nasa:pds:system_bundle:xml_schema:pds-xml_schema
MAVEN Mission Schema, v. 1.0	MAVEN	
MAVEN Mission Schematron, v. 1.0	MAVEN	

3.1 Data Processing Levels

A number of different systems may be used to describe data processing level. This document refers to data by their PDS4 processing level. Table 8 provides a description of these levels along with the equivalent designations used in other systems.

Table 8: Data processing level designations

PDS4 processing level	PDS4 processing level description	MAVEN Processing Level	CODMAC Level	NASA Level
Raw	Original data from an instrument. If compression, reformatting, packetization, or other translation has been applied to facilitate data transmission or storage, those processes are reversed so that the archived data are in a PDS approved archive format.	0	2	1A
Reduced	Data that have been processed beyond the raw stage but which are not yet entirely independent of the instrument.	1	2	1A
Calibrated	Data converted to physical units entirely independent of the instrument.	2	3	1B

PDS4 processing level	PDS4 processing level description	MAVEN Processing Level	CODMAC Level	NASA Level
Derived	Results that have been distilled from one or more calibrated data products (for example, maps, gravity or magnetic fields, or ring particle size distributions). Supplementary data, such as calibration tables or tables of viewing geometry, used to interpret observational data should also be classified as 'derived' data if not easily matched to one of the other three categories.	3+	4+	2+

3.2 Products

A PDS product consists of one or more digital and/or non-digital objects, and an accompanying PDS label file. Labeled digital objects are data products (i.e. electronically stored files). Labeled non-digital objects are physical and conceptual entities which have been described by a PDS label. PDS labels provide identification and description information for labeled objects. The PDS label defines a Logical Identifier (LID) by which any PDS labeled product is referenced throughout the system. In PDS4 labels are XML formatted ASCII files. More information on the formatting of PDS labels is provided in Section 0. More information on the usage of LIDs and the formation of MAVEN LIDs is provided in Section 5.1.

3.3 Product Organization

The highest level of organization for PDS archive is the bundle. A bundle is a list of one or more related collection products which may be of different types. A collection is a list of one or more related basic products which are all of the same type. Figure 13 below illustrates these relationships.

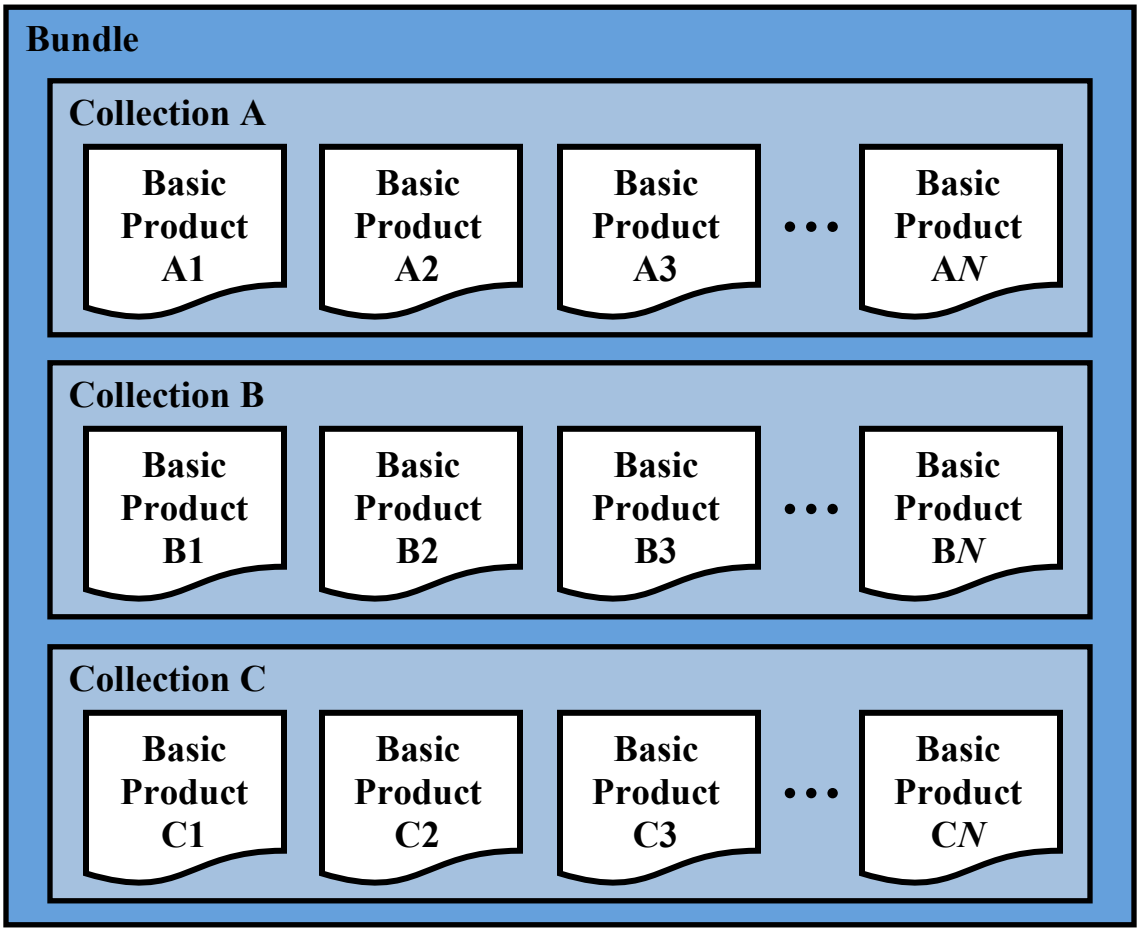

Figure 13: A graphical depiction of the relationship among bundles, collections, and basic products.

Bundles and collections are logical structures, not necessarily tied to any physical directory structure or organization. Bundle and collection membership is established by a member inventory list. Bundle member inventory lists are provided in the bundle product labels themselves. Collection member inventory lists are provided in separate collection inventory table files. Sample bundle and collection labels are provided in Appendix C and Appendix D, respectively.

3.3.1 Collection and Basic Product Types

Collections are limited to a single type of basic products. The types of archive collections that are defined in PDS4 are listed in Table 9.

Table 9: Collection product types

Collection Type	Description
Browse	Contains products intended for data characterization, search, and viewing, and not for scientific research or publication.
Calibration	Contains data and files necessary for the calibration of basic products.
Context	Contains products which provide for the unique identification of objects which form the context for scientific observations (*e.g.* spacecraft, observatories, instruments, targets, etc.).
Document	Contains electronic document products which are part of the PDS Archive.
Data	Contains scientific data products intended for research and publication.
SPICE	Contains NAIF SPICE kernels.
XML_Schema	Contains XML schemas and related products which may be used for generating and validating PDS4 labels.

3.4 Bundle Products

The SWEA data archive is organized into one bundle. A description of the bundle is provided in Table 10, and a more detailed description of the contents and format is provided in Section 5.2.

Table 10: SWEA Bundle

Bundle Logical Identifier	PDS4 Reduction Level	Description	Data Provider
urn:nasa:pds:maven.swea.calibrated	Calibrated	Fully calibrated electron energy/angle (3D) distributions, pitch angle distributions, and omni-directional energy spectra. Tables of sensitivity and energy/angle maps included in files.	ITF

3.5 Data Flow

This section describes only those portions of the MAVEN data flow that are directly connected to archiving. A full description of MAVEN data flow is provided in the MAVEN Science Data Management Plan [5]. A graphical representation of the full MAVEN data flow is provided in Fig. 14.

Reduced (MAVEN level 1) data will be produced by RS and NGIMS as an intermediate processing product, and are delivered to the SDC for archiving at the PDS, but will not be used by the MAVEN team.

All ITFs will produce calibrated products. Following an initial 2-month period at the beginning of the mapping phase, the ITFs will routinely deliver preliminary calibrated data products to the SDC for use by the entire MAVEN team within two weeks of ITF receipt of all data needed to generate those products. The SOC will maintain an active archive of all MAVEN science data, and will provide the MAVEN science team with direct access through the life of the MAVEN mission. After the end of the MAVEN project, PDS will be the sole long-term archive for all public MAVEN data.

Updates to calibrations, algorithms, and/or processing software are expected to occur regularly, resulting in appropriate production system updates followed by reprocessing of science data products by ITFs for delivery to SDC. Systems at the SOC, ITFs and PDS are designed to handle these periodic version changes.

Data bundles intended for the SWEA archive are identified in Table 10.

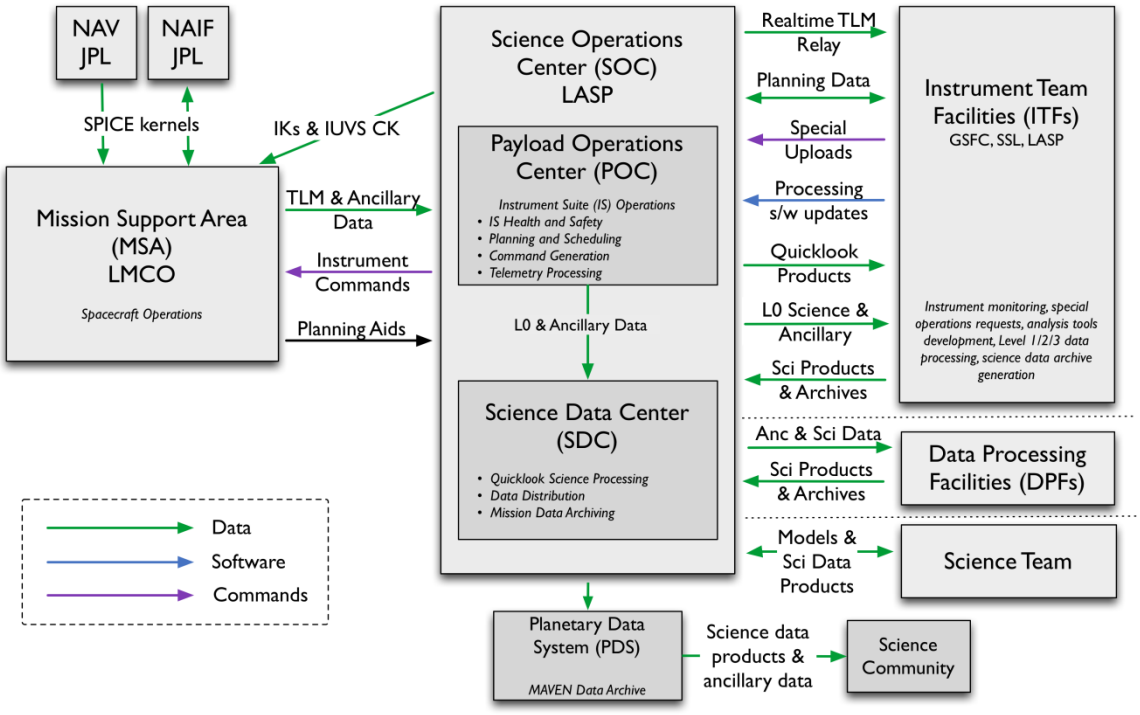

Figure 14: MAVEN Ground Data System responsibilities and data flow. Note that this figure includes portions of the MAVEN GDS which are not directly connected with archiving, and are therefore not described in Section 3.5 above.

4 Archive Generation

The SWEA archive products are produced by the SWEA team in cooperation with the SDC, and with the support of the PDS Planetary Plasma Interactions (PPI) Node at the University of California, Los Angeles (UCLA). The archive volume creation process described in this section sets out the roles and responsibilities of each of these groups. The assignment of tasks has been agreed upon by all parties. Archived data received by the PPI Node from the SWEA team are made available to PDS users electronically as soon as practicable but no later two weeks after the delivery and validation of the data.

4.1 Data Processing and Production Pipeline

The following sections describe the process by which data products in the SWEA bundle listed in Table 10 are produced. All levels refer to MAVEN processing levels (Table 8).

4.1.1 Raw Data Production Pipeline

After receiving Level 0 data from the POC, the SDC will process the Level 0 into Quicklook science products using software provided by the SWEA ITF. The SDC will provide the SWEA ITF with Level 0 data files (consisting of compressed PF packets in their native format, one file per UT day for all PF Survey data, and one file per UT day for all PF Archive data), Quicklook science data, and all ancillary data required for science processing. From these data, the SWEA ITF will generate Level 2 calibrated science data products. The science data products that the SWEA ITF delivers to the SDC will be stored by the SDC for the duration of the project, and will be made available to the MAVEN team. The SDC will deliver archival-quality science data products to the PDS for distribution to the public and long-term archiving in accordance with the SWEA-PDS SIS (this document) and the SOC-PDS SIS. The SDC will also be responsible for delivering Level 0 archives and non-SPICE ancillary data to the PDS for long-term archiving, in accordance with the SOC-PDS SIS and the Export Control Checklist.

4.1.2 Calibrated Data Production Pipeline

Calibrated SWEA Level 2 data will be produced from the raw level 0 PF data files by the SWEA ITF using IDL software, and provided for archiving in the PDS in CDF format. The data production pipeline will be run in an automated fashion to produce archival-ready files from the raw level 0 data.

Beginning as soon as possible but no later than 2 months after the start of science operations, the SWEA ITF will routinely generate Level 2 science data products and deliver them to the SOC. After the initial 2-month calibration period, the SWEA ITF will deliver preliminary Level 2 products to the SDC for distribution to the MAVEN team within two weeks of receiving all data required for science processing (including all SPICE kernels and other ancillary data required for processing) by the ITFs. Final Level 2 SWEA products will be delivered to the SDC as soon as they are complete, no later than needed to meet the PDS delivery schedule in Table 12.

The SWEA ITF does not plan to produce Level 3 products, instead using Level 2 as the final science products.

The SWEA ITF will deliver validated science data products and associated metadata for PDS archiving to the SOC two weeks prior to every PDS delivery deadline. The first PDS delivery will occur no later than 6 months after the start of science operations, and subsequent deliveries will take place every 3 months after the first delivery. The first delivery will include data

collected during the cruise and transition phases in addition to the science data from the first 3 months of the mapping phase. Each subsequent delivery will contain data from the 3 months following the previous delivery. The final delivery may contain products involving data from the entire mission.

The SWEA ITF will also provide the SDC with data product descriptions, appropriate for use by the MAVEN science team in using MAVEN science data products and consistent with PDS metadata standards.

4.2 Data Validation

4.2.1 Instrument Team Validation

All SWEA data will be calibrated and converted to physical units by the SWEA ITF, then spot-checked by the instrument lead and his designees for accuracy and integrity.

4.2.2 MAVEN Science Team Validation

The MAVEN science team will work with the same SWEA products that will be archived in the PDS. If any calibration issues or other anomalies are noted, they will be addressed at the SWEA ITF by the instrument lead or his designees.

4.2.3 PDS Peer Review

The PPI node will conduct a full peer review of all of the data types that the SWEA team intends to archive. The review data will consist of fully formed bundles populated with candidate final versions of the data and other products and the associated metadata.

Table 11: MAVEN PDS review schedule

Date	Activity	Responsible Team
2014-Mar-24	Signed SIS deadline	ITF
2014-Apr-18	Sample data products due	ITF
2014-May to 2014-Aug	Preliminary PDS Peer Review (SIS, sample data files)	PDS
2015-Mar-02	Release #1: Data due to PDS	ITF/SDC
2014-Mar to 2015-Apr	Release #1: Data PDS Peer Review	PDS
2015-May-01	Release #1: Public release	PDS

Reviews will include a preliminary delivery of sample products for validation and comment by PDS PPI and Engineering node personnel. The data provider will then address the comments coming out of the preliminary review, and generate a full archive delivery to be used for the peer review.

Reviewers will include MAVEN Project and SWEA team representatives, researchers from outside of the MAVEN project, and PDS personnel from the Engineering and PPI nodes. Reviewers will examine the sample data products to determine whether the data meet the stated science objectives of the instrument and the needs of the scientific community and to verify that the accompanying metadata are accurate and complete. The peer review committee will identify any liens on the data that must be resolved before the data can be 'certified' by PDS, a process by which data are made public as minor errors are corrected.

In addition to verifying the validity of the review data, this review will be used to verify that the data production pipeline by which the archive products are generated is robust. Additional deliveries made using this same pipeline will be validated at the PPI node, but will not require additional external review.

As expertise with the instrument and data develops the SWEA team may decide that changes to the structure or content of its archive products are warranted. Any changes to the archive products or to the data production pipeline will require an additional round of review to verify that the revised products still meet the original scientific and archival requirements or whether those criteria have been appropriately modified. Whether subsequent reviews require external reviewers will be decided on a case-by-case basis and will depend upon the nature of the changes. A comprehensive record of modifications to the archive structure and content is kept in the Modification_History element of the collection and bundle products.

The instrument team and other researchers are encouraged to archive additional SWEA products that cover specific observations or data-taking activities. The schedule and structure of any additional archives are not covered by this document and should be worked out with the PPI node.

4.3 Data Transfer Methods and Delivery Schedule

The SOC is responsible for delivering data products to the PDS for long-term archiving. While ITFs are primarily responsible for the design and generation of calibrated and derived data archives, the archival process is managed by the SOC. The SOC (in coordination with the ITFs) will also be primarily responsible for the design and generation of the raw data archive. The first PDS delivery will take place within 6 months of the start of science operations. Additional deliveries will occur every following 3 months and one final delivery will be made after the end of the mission. Science data are delivered to the PDS within 6 months of its collection. If it becomes necessary to reprocess data which have already been delivered to the archive, the ITFs will reprocess the data and deliver them to the SDC for inclusion in the next archive delivery. A summary of this schedule is provided in Table 12 below.

Table 5: Archive bundle delivery schedule

Bundle Logical Identifier	First Delivery to PDS	Delivery Schedule	Estimated Delivery Size
urn:nasa:pds:maven.swea.calibrated	No later than 6 months after the start of science operations	Every 3 months	11.8 GB

Each delivery will comprise both data and ancillary data files organized into directory structures consistent with the archive design described in Section 5, and combined into a deliverable file(s) using file archive and compression software. When these files are unpacked at the PPI Node in the appropriate location, the constituent files will be organized into the archive structure.

Archive deliveries are made in the form of a “delivery package”. Delivery packages include all of the data being transferred along with a transfer manifest, which helps to identify all of the products included in the delivery, and a checksum manifest which helps to insure that integrity of the data is maintained through the delivery. The format of these files is described in Section 6.4.

Data are transferred electronically (using the *ssh* protocol) from the SOC to an agreed upon location within the PPI file system. PPI will provide the SOC a user account for this purpose. Each delivery package is made in the form of a compressed *tar* or *zip* archive. Only those files that have changed since the last delivery are included. The PPI operator will decompress the data, and verify that the archive is complete using the transfer and MD5 checksum manifests that were included in the delivery package. Archive delivery status will be tracked using a system defined by the PPI node.

Following receipt of a data delivery, PPI will reorganize the data into its PDS archive structure within its online data system. PPI will also update any of the required files associated with a PDS archive as necessitated by the data reorganization. Newly delivered data are made available

publicly through the PPI online system once accompanying labels and other documentation have been validated. It is anticipated that this validation process will require no more than fourteen working days from receipt of the data by PPI. However, the first few data deliveries may require more time for the PPI Node to process before the data are made publicly available.

The MAVEN prime mission begins approximately 5 weeks following MOI and lasts for 1 Earth-year. Table 12 shows the data delivery schedule for the entire mission.

4.4 Data Product and Archive Volume Size Estimates

SWEA data products consist of files that span one UT day, breaking at 0h UTC SCET. Files vary in size depending on the telemetry rate and allocation.

4.5 Data Validation

Routine data deliveries to the PDS are validated at the PPI node to ensure that the delivery meets PDS standards, and that the data conform to the SIS as approved in the peer review. As long as there are no changes to the data product formats, or data production pipeline, no additional external review will be conducted.

4.6 Backups and duplicates

The PPI Node keeps three copies of each archive product. One copy is the primary online archive copy, another is an onsite backup copy, and the final copy is an off-site backup copy. Once the archive products are fully validated and approved for inclusion in the archive, copies of the products are sent to the National Space Science Data Center (NSSDC) for long-term archive in a NASA-approved deep-storage facility. The PPI Node may maintain additional copies of the archive products, either on or off-site as deemed necessary. The process for the dissemination and preservation of SWEA data is illustrated in Figure 15.

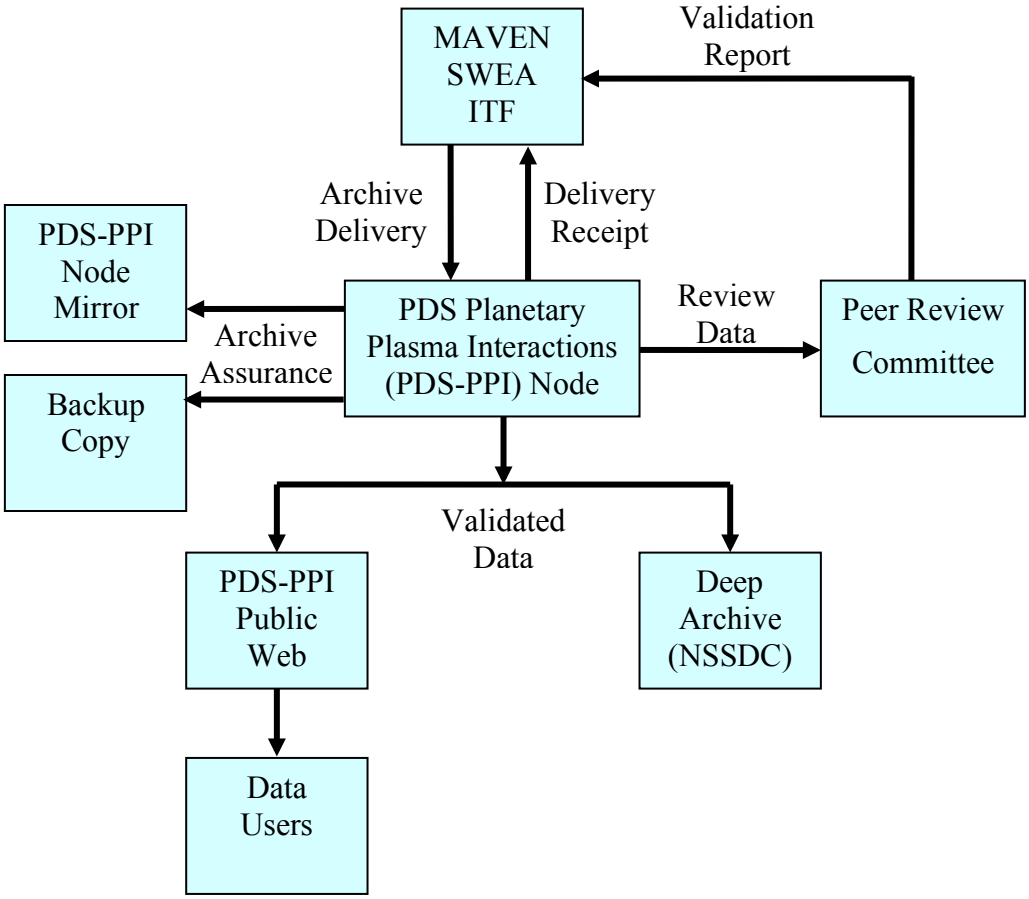

Figure 15: Duplication and dissemination of SWEA archive products at PDS/PPI.

5 Archive organization and naming

This section describes the basic organization of an SWEA bundle, and the naming conventions used for the product logical identifiers, and bundle, collection, and basic product filenames.

5.1 Logical Identifiers

Every product in PDS is assigned an identifier which allows it to be uniquely identified across the system. This identifier is referred to as a Logical Identifier or LID. A LIDVID (Versioned Logical Identifier) includes product version information, and allows different versions of a specific product to be referenced uniquely. A product's LID and VID are defined as separate attributes in the product label. LIDs and VIDs are assigned by the entity generating the labels and are formed according to the conventions described in sections 5.1.1 and 5.1.2 below. The uniqueness of a product's LIDVID may be verified using the PDS Registry and Harvest tools.

5.1.1 LID Formation

LIDs take the form of a Uniform Resource Name (URN). LIDs are restricted to ASCII lower case letters, digits, dash, underscore, and period. Colons are also used, but only to separate prescribed components of the LID. Within one of these prescribed components dash, underscore, or period are used as separators. LIDs are limited in length to 255 characters.

MAVEN SWEA LIDs are formed according to the following conventions:

- Bundle LIDs are formed by appending a bundle specific ID to the MAVEN SWEA base ID:

  urn:nasa:pds:maven.swea.<bundle ID>

  Since all PDS bundle LIDs are constructed this way, the combination of maven.swea.bundle must be unique across all products archived with the PDS.

- Collection LIDs are formed by appending a collection specific ID to the collection's parent bundle LID:

  urn:nasa:pds:maven.swea.<bundle ID>:<collection ID>

  Since the collection LID is based on the bundle LID, which is unique across PDS, the only additional condition is that the collection ID must be unique across the bundle. Collection IDs correspond to the collection type (e.g. "browse", "data", "document", etc.). Additional descriptive information may be appended to the collection type (e.g. "data-raw", "data-calibrated", etc.) to insure that multiple collections of the same type within a single bundle have unique LIDs.

- Basic product LIDs are formed by appending a product specific ID to the product's parent collection LID:

  urn:nasa:pds:maven.swea.<bundle ID>:<collection ID>:<product ID>

  Since the product LID is based on the collection LID, which is unique across PDS, the only additional condition is that the product ID must be unique across the collection.

A list of SWEA bundle LIDs is provided in Table 10. Collection LIDs are listed in Table 13.

5.1.2 VID Formation

Product version ID's consist of major and minor components separated by a "." (M.n). Both components of the VID are integer values. The major component is initialized to a value of "1", and the minor component is initialized to a value of "0". The minor component resets to "0" when the major component is incremented.

5.2 SWEA Archive Contents

The SWEA archive includes the calibrated (MAVEN Level 2) bundle listed in Table 10. The following sections describe the contents of each of these bundles in greater detail.

5.2.1 SWEA Calibrated (MAVEN Level 2) Science Data Bundle

The swea.calibrated Level 2 Science Data Bundle contains fully calibrated data in physical units, consisting of energy/angle (3D) distributions, pitch angle distributions (PADs), and omni-directional energy spectra.

Table 6: swea.calibrated Level 2 Science Data Collections

Collection LID	Description
urn:nasa.pds:maven.swea.calibrated:data.svy_3d	Energy/angle (3D) distributions in units of differential energy flux (eV/cm^2 sec ster eV) from SWEA survey data
urn:nasa.pds:maven.swea.calibrated:data.arc_3d	Energy/angle (3D) distributions in units of differential energy flux (eV/cm^2 sec ster eV) from SWEA archive data
urn:nasa.pds:maven.swea.calibrated:data.svy_pad	Pitch angle distributions in units of differential energy flux (eV/cm^2 sec ster eV) from SWEA survey data
urn:nasa.pds:maven.swea.calibrated:data.arc_pad	Pitch angle distributions in units of differential energy flux (eV/cm^2 sec ster eV) from SWEA archive data
urn:nasa.pds:maven.swea.calibrated:data.svy_spec	Omni-directional energy spectra in units of differential energy flux (eV/cm^2 sec ster eV) from SWEA survey data
urn:nasa.pds:maven.swea.calibrated:data.arc_spec	Omni-directional energy spectra in units of differential energy flux (eV/cm^2 sec ster eV) from SWEA archive data
urn:nasa:pds:maven.swea.calibrated:document	Documents related to the swea.calibrated bundle.

5.2.1.1 swea.calibrated.svy_3d Data Collection

SWEA survey 3D collections contain files with time-ordered arrays of raw counts and fully calibrated electron energy/angle distributions in units of differential energy flux (eV/cm^2 sec ster eV). Ancillary information needed to interpret the data is also provided.

The data files contain a time-ordered array with three time scales: Epoch time, Mission Elapsed Time (MET) and Unix time. All times refer to the center of the accumulation interval for each

data record. Epoch time is a 64-bit signed integer defined as terrestrial time with a time base of J2000 (Julian date 2451545.0 TT or 2000 January 1, 12h TT) in units of nanoseconds. This time reference, known as TT2000, accounts for leap seconds. Conversion between TT and UTC is straightforward: TT = UTC + deltaAT + 32.184s, where deltaAT is the sum of the leap seconds since 1960. Unix time is a double precision float that is the number of seconds (including fractional seconds) since 00:00:00 UTC on January 1, 1970, not counting leap seconds. MET is the same as spacecraft clock time (SCLK), except that the units of MET are seconds, and SCLK is in units of the smallest time increment of the spacecraft clock, which for MAVEN is 1/65536 sec. MET is the primary data collection reference for the entire MAVEN payload. (The 2-second SWEA data collection cycle is synchronized to MET.) A correction for spacecraft clock drift is performed when converting MET to TT2000 and Unix time.

At each time step, data are packaged into a 64-energy × 16-azimuth angle × 6-elevation angle array[1], with an energy binning factor (1 = 64 energies, 2 = 32 binned energies, 4 = 16 binned energies). For data with 32 or 16 binned energies, a full 64-energy data structure is provided for commonality and ease of use, but the 64 energy steps contain the binned counts duplicated B times (B = 2 or 4). For example, for a case with 16 binned energy steps (B = 4), each of the first four of the 64 energies contain the total number of counts in the first binned energy step. (Duplicated bins have an effective integration time that is B times longer than for un-duplicated bins.) The energy array contains the original 64 energies of the sweep, before any summing or duplication of counts. Thus, the effective energy of the summed bins can be computed after the fact. If the spectrum is steeply rising or falling with energy, the original distribution of counts among the summed bins would be highly non-uniform. This is a general feature of any binning scheme, whether performed by the instrument, in flight software, or on the ground. The re-binning scheme ensures that moments or other sums computed from binned data still come out right, and use of 3D data with different binning schemes is transparent to the end user. However, case must be taken when calculating statistical uncertainties, since duplicated bins are not independent.

The data files contain a 64-element list of energies, a 64×6-element array of elevation angles, a 64×6-element array of relative elevation sensitivities, a 16-element array of azimuth angles, a 16-element array of relative anode sensitivities, and an integration time, for use with the 3D data products. The files also contain the energy resolution of the sweep tables and the full sensor geometric factor. All of these support data are stored as NOVARY records, meaning they are the same for all times in the file.

To convert between raw counts and differential energy flux, first calculate the raw count rate per anode:

$$R' = \frac{\text{COUNTS}}{\text{BINNING} \times \text{ACCUM\_TIME}}$$

[1] Array dimensions are listed in column-major format. This is the same as in the column-major programming languages IDL and Fortran. Row-major languages, such as Matlab and C, will represent this same array in reverse order (6 × 16 × 64).

The BINNING term accounts for the summing of adjacent energy channels. For the 3D data product, this term must be multiplied by an additional factor of 2 at the highest positive and negative elevations to account for the summing of adjacent azimuth sectors at those elevations. This applies to the 3D data product only.

Next, correct for dead time:

$$R = R'(1 - R'\tau)^{-1}$$

where $\tau = 2.8 \times 10^{-6}$ sec is the dead time for one of the 16 MCP-anode-preamp chains. Data are flagged as bad whenever $R' > 0.8/\tau$.

Finally, convert to differential energy flux (eV/cm^2-sec-ster-eV):

$$\text{DIFF\_EN\_FLUX} = \frac{\text{R}}{\text{GEOM\_FACTOR} \times \text{G\_ENGY} \times \text{G\_AZIM} \times \text{G\_ELEV}}$$

The terms in the denominator are as follows:

GEOM_FACTOR: The geometric factor per anode sector from ground calibrations with a beam energy of 1.4 keV and V_0 disabled (inner toroidal grid held at ground throughout the sweep). This calibration was performed on the fully assembled analyzer, so it includes the overall MCP efficiency at 1.4 keV (typically ~75%). Units are cm^2-ster-eV/eV.

G_ENGY: Sensitivity variation with energy. This is composed of two multiplicative terms. The first is variation of the MCP efficiency with energy (Goruganthu and Wilson, *Rev. Sci. Instr.* **55**, 2030, 1984), and the second is variation of the geometric factor with energy when using the V_0 operation mode (see Section 2). Dimensionless. When V_0 is disabled, G_ENGY is normalized to unity at 1.4 keV.

G_AZIM: Sensitivity variation with azimuth due to MCP efficiency variations and geometric blockage from support ribs. Dimensionless; average normalized to unity.

G_ELEV: Sensitivity variation with elevation (mostly due to optics). Dimensionless; average normalized to unity.

When energy and/or azimuth bins are duplicated, the linear average of G_ENGY and/or G_AZIM is recorded for each group of duplicated values. All 64 energies are always recorded in ENERGY with no averaging. The BINNING factor can be used to determine the energies of the bins that have been summed.

The 3D data product can be compared with the SPEC data product (see below) by summing over the 96 solid angle bins, each weighted by solid angle, and then dividing by the total solid angle subtended by the FOV, thus maintaining units of eV/cm^2-sec-ster-eV (see Section 2.3.3).

Figure 16 shows an example of the 3D data product, summed over a 6.4-minute interval during which the magnetic field direction was nearly constant. This distribution was measured in the solar wind at an altitude of 6100 km. At an energy of 125 eV (shown here), the distribution is

dominated by the solar wind halo population, which is typically beamed away from the Sun along the interplanetary magnetic field. This beam can be seen clearly in the angular distribution centered on the –B direction. Ten of the 96 solid angle bins are masked because of spacecraft blockage. Since the spacecraft is fixed in SWEA's field of view, the same bins (0-3, 14-18, and 31) are always marked as invalid (NaN) in the 3D data product.

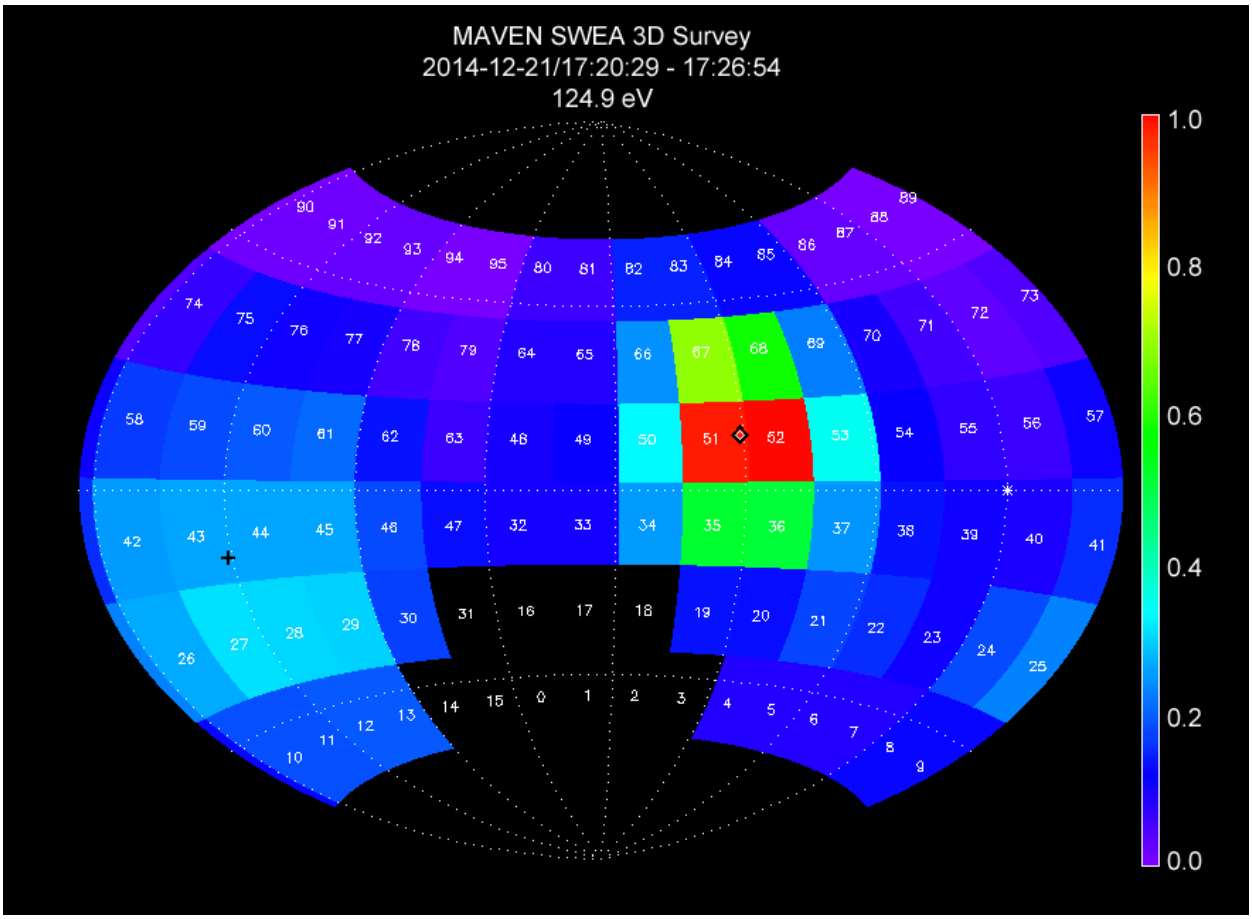

Figure 16: SWEA 3D data product showing the angular distribution of 125-eV electrons in the solar wind. The data are normalized to unity at the peak energy flux, and relative variations are shown with a linear color scale. The data are mapped in instrument coordinates over the full sky with an Aitoff projection, and each azimuth-elevation bin is labeled with its bin number (0-95). The instrument's blind spots (|elevation| > 60°) and bins blocked by the spacecraft have no color. The magnetic field direction is indicated by the plus (+B) and diamond (–B) symbols.

The SWEA ITF will produce these products, with one file per UT day, with the naming convention mvn_swe_l2_svy3d_<yyyy><mm><dd>_v<xx>_r<yy>.cdf, where:

<yyyy> = Four digit year.

<mm> = Two digit month (e.g., 01, 12).

<dd> = Two digit day of month (e.g., 01, 31).

v<xx> = Major revision number. This number changes with a significant change in the processing algorithm or instrument calibration parameters. Typically, a change in major revision

triggers a reprocessing of the entire data set. Changes to the major revision are controlled by the corresponding instrument lead and are documented.

r<yy> = Minor revision number. This number changes whenever the data are regenerated without a change to the major revision. This can occur for a variety of reasons, typically to fill in missing science data or to apply new or updated ancillary data, such as SPICE kernels.

The complete file naming convention (Appendix B) includes optional fields, which are not used by SWEA. All data records have time tags between 00:00:00 and 23:59:59 (or 23:59:60 if on a leap second) of the date specified. All time tags correspond to the center of the accumulation interval.

5.2.1.2 swea.calibrated.arc_3d Data Collection

SWEA archive 3D collections are identical to SWEA survey 3D collections, as described in the previous section. The only difference is the naming convention:

mvn_swe_l2_arc3d_<yyyy><mm><dd>_v<xx>_r<yy>.cdf

Archive data have higher energy and/or time resolution, but for limited spans of time.

5.2.1.3 swea.calibrated.svy_pad Data Collection

SWEA survey PAD collections contain files with time-ordered fully calibrated electron pitch angle distributions in units of differential energy flux (eV/cm^2 sec ster eV) derived from the SWEA PAD survey telemetry, as well as a header of ancillary information needed to interpret the data.

The data files contain a time-ordered array with time in Epoch time, Mission-Elapsed-Time (MET) and Unix time (Seconds since 1970-01-01/00:00), a 64-energy × 16-pitch angle array of data, and the energy binning factor (1 = 64 energies, 2 = 32 binned energies, 4 = 16 binned energies) at each time step.

For data with 32 or 16 binned energies, a full 64-energy data structure is provided for commonality and ease of use, but the 64 energy steps contain the binned counts duplicated B times (B = 2 or 4). For example, for a case with 16 binned energy steps (B = 4), each of the first four steps of the 64 energies contain the number of counts in the first binned energy step. (Duplicated bins have an effective integration time that is B times longer than for un-duplicated bins.) This re-binning scheme ensures that use of PAD data with different binning schemes is transparent to the end user. However, case must be taken when calculating statistical uncertainties, since duplicated bins are not independent.

The mapping of pitch angle around the field of view varies with time as the magnetic field direction changes. For each PAD measurement, flight software applies a nominal calibration (fixed gains and offsets) to the raw magnetic field data and estimates the magnetic field direction in SWEA instrument coordinates. With this information, it determines the optimal 2D cut (great circle) through the 3D distribution that includes the magnetic field direction, or comes as close as possible to doing so while staying entirely within the instrument's field of view. The PAD data files contain the magnetic field azimuth and elevation (B_AZIM, B_ELEV), in instrument coordinates, used by flight software to perform this calculation.

Each of the 16 pitch angle bins in the PAD data product maps directly into one of the 96 solid angle bins in the 3D data product, without averaging or interpolation. Consequently, the pitch angle map can be refined in ground processing using fully calibrated Level 2 Magnetometer data. The data files contain a 64×16-element array of pitch angles (PA) and a 64×16-element array of pitch angle ranges (D_PA; full width centered at each pitch angle) that are calculated from Level 2 Magnetometer data, as well as relative sensitivity variations in azimuth and elevation as mapped into pitch angle (G_PA). All of these vary with time.

The files also contain support data that do not vary with time: 64-element arrays of bin energies (ENERGY) and energy resolution (ΔE/E, FWHM), the geometric factor per anode sector measured at 1.4 keV (GEOM_FACTOR), and a 64-element array that provides relative sensitivity variations with energy (G_ENGY). Finally, the files contain the accumulation time per sample. All of these support data are stored as /novary records in the CDF files.

To convert between raw counts and differential energy flux, use the same procedure as for the 3D distributions, except the product (G_AZIM × G_ELEV) is replaced by G_PA. There is no summing of azimuth bins at high elevations for the PAD data product, so only the energy binning factor applies.

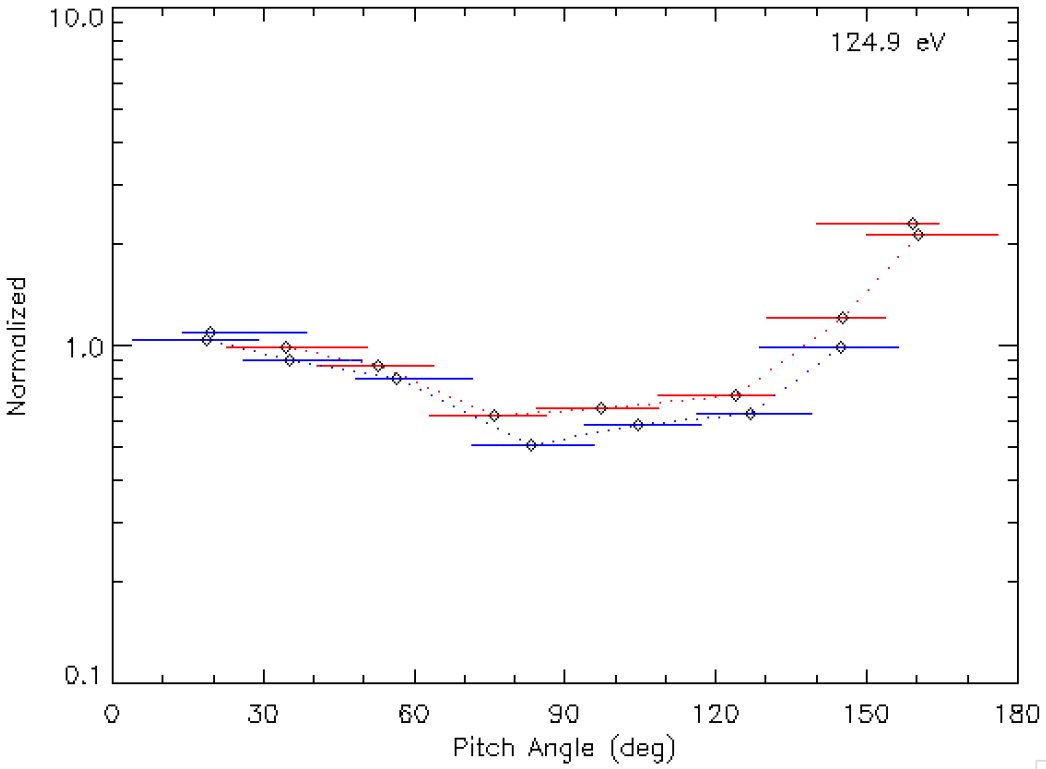

Figure 17: Electron pitch angle distribution measured in the solar wind over the same time interval in Fig. 16. The distribution is measured twice (blue and red), and the pitch angle coverage of each bin is indicated by the horizontal bar. This cut through the 3D distribution does not intersect the spacecraft, so all 16 pitch angle bins represent valid measurements. When a cut does include 3D bins that are blocked by the spacecraft, those bins are flagged as invalid (NaN) in the PAD data.

Figure 17 shows an electron pitch angle distribution measured over the same time interval as the 3D distribution in Fig. 16. Because SWEA has 360-degree coverage in azimuth, the 0-180-degree pitch angle distribution is measured twice. The field-aligned beam appears in the pitch angle distribution as an increased flux from ~150 to 180 degrees.

The SWEA ITF will produce these products, with one file per UT day, with the naming convention mvn_swe_l2_svypad_<yyyy><mm><dd>_v<xx>_r<yy>.cdf

5.2.1.4 swea.calibrated.arc_pad Data Collection

SWEA archive PAD collections are identical to SWEA survey PAD collections, as described in the previous section. The only difference is the naming convention:

mvn_swe_l2_arcpad_<yyyy><mm><dd>_v<xx>_r<yy>.cdf

Archive data have higher energy and/or time resolution, but for limited spans of time.

5.2.1.5 swea.calibrated.svy_spec Data Collection

SWEA survey SPEC collections contain files with time-ordered angle-averaged electron energy spectra in units of differential energy flux (eV/cm^2 sec ster eV), as well as a header with ancillary information needed to interpret the spectra.

The data files contain a time-ordered array with time in Epoch time, Mission-Elapsed-Time (MET) and Unix time (Seconds since 1970-01-01/00:00), a 64-element array of angle-averaged differential energy fluxes, and the number of accumulations used to compute the spectra, at each time step.

The data files also contain a 64-element list of energies, and the intrinsic energy resolution of the sweep table, integration time, and geometric factor per anode measured at 1.4 keV. In addition, a weighting factor is included to convert raw counts to raw count rate. All of these support data are stored as /novary records in the CDF files.

To convert between raw counts and differential energy flux, first calculate the raw count rate:

$$R' = \frac{\text{COUNTS}}{\text{WEIGHT\_FACTOR} \times \text{NUM\_ACCUM} \times \text{ACCUM\_TIME}}$$

Since counts are summed over all 16 azimuth and 6 elevation bins, the effective accumulation time is 16×6×4×1.09 msec = 0.418 sec. The term WEIGHT_FACTOR is the average of the six cosθ factors that multiply the raw counts as they are summed onboard (see Section 2.3.3). The term NUM_ACCUM is the number of 2-second accumulations summed per energy spectrum. In sample mode, energy spectra are sampled every 2^N seconds (N = 1, 2, …), and NUM_ACCUM is always unity. In sum mode, energy spectra are summed over 2^N-second intervals, and NUM_ACCUM = 2^{N-1}. This results in a weighted raw count rate per sector (R').

Next, correct for dead time:

$$R = R'(1 - R'\tau)^{-1}$$

Finally, convert to differential energy flux (eV/cm^2-sec-ster-eV):

$$\text{DIFF\_EN\_FLUX} = \frac{\text{R}}{\text{GEOM\_FACTOR} \times \text{G\_ENGY}}$$

The terms in the denominator are as follows:

GEOM_FACTOR: The geometric factor per anode sector from ground calibrations with a beam energy of 1.4 keV and V_0 disabled (inner toroidal grid held at ground throughout the sweep). This calibration was performed on the fully assembled analyzer, so it includes the overall MCP efficiency at 1.4 keV (typically ~75%). Units are cm^2-ster-eV/eV.

G_ENGY: Sensitivity variation with energy. This is composed of two multiplicative terms. The first is variation of the MCP efficiency with energy (Goruganthu and Wilson, *Rev. Sci. Instr.* **55**, 2030, 1984), and the second is variation of the geometric factor with energy when using the V_0 operation mode (see Section 2). Dimensionless. When V_0 is disabled, G_ENGY is normalized to unity at 1.4 keV.

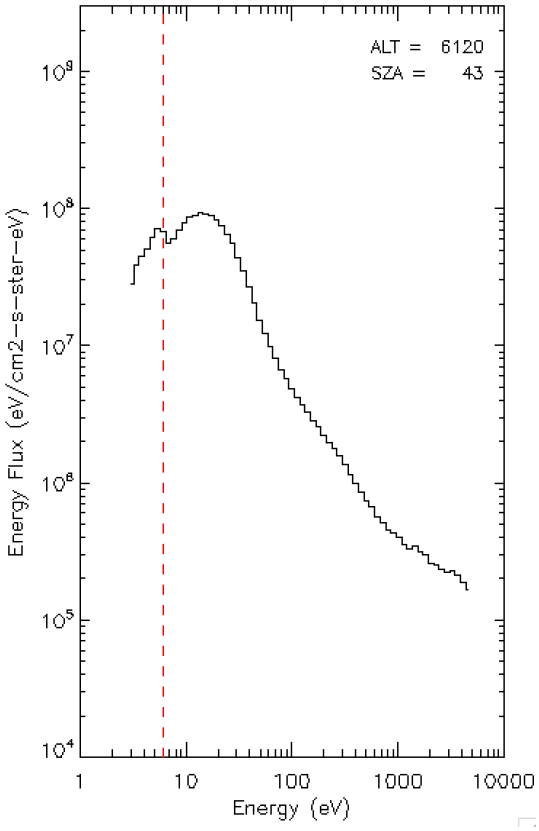

Figure 18: Electron energy distribution measured in the solar wind. The 64 energy channels are logarithmically spaced from 3 eV to 4.6 keV, with a sampling in energy (12%) that is finer than the instrument's intrinsic energy resolution of 17% (ΔE/E, FWHM).

Figure 18 shows an electron energy distribution obtained over the same time interval as in Figs. 16 and 17. The spacecraft potential (+6 Volts, vertical dashed line) can often be identified by a sharp break in the energy distribution. At energies below this potential, SWEA measures spacecraft photoelectrons that have insufficient energy to escape, and are thus attracted back to the spacecraft. At higher energies, SWEA measures ambient solar wind electrons, shifted in energy by the amount of the spacecraft potential.

Removal of spacecraft photoelectrons and correction for spacecraft potential are critical for estimating density and temperature from the measured electron distributions (see the chapter by McFadden *et al.*, in *Calibration of Particle Instruments in Space Physics*, Martin Wuest, David S. Evans, Rudolf von Steiger (eds.), ISSI Scientific Reports Series, p. 277-385, 2007). For example, to estimate electron number density (n_e) from the measured energy flux, we sum over energy and angle:

$$n_e = \left(\frac{m_e}{2}\right)^{1/2} \sum_{\Omega} \sum_{E>\phi} (1 - \phi/E)^{1/2}\, E^{-3/2}\, \mathrm{F}(E, \Omega)\, \Delta E\, \Delta\Omega$$

where E, F, and Ω are the energy, energy flux, and solid angle as measured in the instrument frame; ϕ is the spacecraft potential, and m_e is the electron mass. The sum is carried out only over energy channels above the spacecraft potential. Since SWEA does not measure the distribution over the full sky, this sum is multiplied by a correction factor ($4\pi/\Sigma\Delta\Omega$) to account for the part of the distribution that is not measured, under the assumption that the distribution in the instrument's blind spots is not very different from the part of the distribution that is measured.

The SWEA ITF will produce these products, with one file per UT day, with the naming convention: mvn_swe_l2_svyspec_<yyyy><mm><dd>_v<xx>_r<yy>.cdf

5.2.1.6 swea.calibrated.arc_spec Data Collection

SWEA archive SPEC collections are identical to SWEA survey SPEC collections, as described in the previous section. The only difference is the naming convention:

mvn_swe_l2_arcspec_<yyyy><mm><dd>_v<xx>_r<yy>.cdf

Archive data have higher time resolution, but for limited spans of time.

5.2.1.7 swea.calibrated Document Collection

The SWEA calibrated data document collection contains documents which are useful for understanding and using the SWEA Calibrated (MAVEN Level 2) Science Data bundle. Table 14 contains a list of the documents included in this collection, along with the LID, and responsible group. Following this a brief description of each document is also provided.

Table 14: SWEA Calibrated Science Data Documents

Document Name	LID	Responsiblility
MAVEN Science Data Management Plan	urn:nasa:pds:maven:document:sdmp	MAVEN Project
MAVEN SWEA Archive SIS	urn:nasa:pds:maven.swea:document:SIS	SWEA Team
MAVEN SWEA Instrument Paper	urn:nasa:pds:maven.swea:document: swea.instpaper	SWEA Team

MAVEN Science Data Management Plan – describes the data requirements for the MAVEN mission and the plan by which the MAVEN data system will meet those requirements

MAVEN SWEA Archive SIS – describes the format and content of the SWEA PDS data archive, including descriptions of the data products and associated metadata, and the archive format, content, and generation pipeline (this document)

SWEA Instrument Paper – describes the instrument operation and data products.

While responsibility for the individual documents varies, the document collection itself is managed by the PDS/PPI node.

6 Archive product formats

Data that comprise the SWEA archives are formatted in accordance with PDS specifications [see *Planetary Science Data Dictionary* [4], *PDS Data Provider's Handbook* [2], and *PDS Standards Reference* [3]. This section provides details on the formats used for each of the products included in the archive.

6.1 Data File Formats

This section describes the format and record structure of each of the data file types.

6.1.1 Calibrated data file structure

SWEA calibrated data files will be archived with PDS as Common Data Format (CDF). In order to allow the archival CDF files to be described by PDS metadata a number of requirements have been agreed to between the SWEA ITF and the PDS-PPI node. An early version of these requirements are detailed in the document *Archive of MAVEN CDF in PDS4* (T. King and J. Mafi, July 16, 2013). All parties will agree upon the final requirements before sample files are produced. These CDF files will be the same ones used and distributed by the SWEA ITF internally. The contents of the SWEA CDF files are described in the tables below.

Table 7: Contents for swea.calibrated.svy_3d and swea.calibrated.arc_3d data files

Field Name	Data Type	Description
EPOCH	TT2000 (64-bit signed integer)	UTC time from 01-Jan-2000 12:00:00.000 including leap seconds, one element per 3D distribution (NUM_DISTS elements)
TIME_MET	DOUBLE (64-bit float)	Mission elapsed time (spacecraft clock or SCLK in SPICE terms) for this data record, one element per 3D distribution (NUM_DISTS elements)
TIME_UNIX	DOUBLE (64-bit float)	Unix time (elapsed seconds since 1970-01-01/00:00 without leap seconds) for this data record, one element per 3D distribution (NUM_DISTS elements)
BINNING	INTEGER (8-bit signed integer)	Energy binning factor, B (1 = 64 energies, 2 = 32 energies, 4 = 16 energies), one element per 3D distribution (NUM_DISTS elements). Duplicated bins have an effective integration time that is B times longer than for unduplicated bins. At the highest positive and negative elevations, this binning factor must be multiplied by 2 to account for the summing of adjacent azimuth bins.
COUNTS	FLOAT (32-bit float)	64×16×6-element array of 3D product counts, one array per 3D distribution (NUM_DISTS×64×16×6 elements). When adjacent energy and/or azimuth bins are summed, the raw counts are duplicated among the summed bins, and the binning factor is used to renormalize when computing count rate.

DIFF_EN_FLUXES	FLOAT (32-bit float)	64×16×6-element array of differential energy fluxes [eV/(cm^2 s sr eV)] computed from the COUNTS array, as described above.
GEOM_FACTOR	FLOAT (NOVARY) (32-bit float)	Geometric factor per anode [cm^2 s sr eV/eV] measured at 1.4 keV. This includes a factor for the overall MCP efficiency at 1.4 keV.
G_ENGY	FLOAT (NOVARY) (32-bit float)	64-element array of relative sensitivity as a function of energy. This accounts for the energy dependence of the MCP efficiency, as well as the effects of using V_0.
DE_OVER_E	FLOAT (NOVARY) (32-bit float)	64-element array of energy resolution (FWHM) as a function of energy.
ACCUM_TIME	FLOAT (NOVARY) (32-bit float)	Accumulation time for each sample, nominally 4×1.09 msec to account for the summation over 4 deflection steps for each element of the telemetry product that is used to make the 3D distributions.
ENERGY	FLOAT (NOVARY) (32-bit float)	64-element array of energies (eV) covered by the distribution. All 64 energies are provided, even when B = 2 or 4.
ELEV	FLOAT (NOVARY) (32-bit float)	64×6-element array of elevation angles (instrument coordinates) covered by the distribution
G_ELEV	FLOAT (NOVARY) (32-bit float)	64×6-element array of relative sensitivity as a function of elevation. Average normalized to unity.
AZIM	FLOAT (NOVARY) (32-bit float)	16-element array of azimuth angles (instrument coordinates)
G_AZIM	FLOAT (NOVARY) (32-bit float)	16-element array of relative sensitivity as a function of azimuth. Average normalized to unity.
NUM_DISTS	INTEGER (NOVARY) (32-bit signed integer)	Number of 3D distributions in the file

Table 8: Contents for swea.calibrated.svy_pad and swea.calibrated.arc_pad data files

Field Name	Data Type	Description
EPOCH	TT2000 (64-bit signed integer)	UTC time from 01-Jan-2000 12:00:00.000 including leap seconds, one element per PAD (NUM_DISTS elements)
TIME_MET	DOUBLE (64-bit float)	Mission elapsed time (spacecraft clock or SCLK in SPICE terms) for this data record, one element per PAD (NUM_DISTS elements)
TIME_UNIX	DOUBLE (64-bit float)	Unix time (elapsed seconds since 1970-01-01/00:00 without leap seconds) for this data record, one element per PAD (NUM_DISTS elements)
BINNING	INTEGER (8-bit signed integer)	Energy binning factor, B (1 = 64 energies, 2 = 32 energies, 4 = 16 energies), one element per PAD (NUM_DISTS elements). Duplicated bins have an effective integration time that is B times longer than for unduplicated bins.
COUNTS	FLOAT (32-bit float)	64×16-element array of PAD product counts, one array per PAD distribution (NUM_DISTS×64×16 elements). When adjacent energy bins are summed, the raw counts are duplicated among the summed bins, and the binning factor is used to renormalize when computing count rate.
DIFF_EN_FLUXES	FLOAT (32-bit float)	64×16-element array of differential energy fluxes [eV/(cm^2 s sr eV)] computed from the COUNTS array, as described above.
GEOM_FACTOR	FLOAT (NOVARY) (32-bit float)	Geometric factor per anode [cm^2 s sr eV/eV] measured at 1.4 keV. This includes a factor for the overall MCP efficiency at 1.4 keV.
G_ENGY	FLOAT (NOVARY) (32-bit float)	64-element array of relative sensitivity as a function of energy. This accounts for the energy dependence of the MCP efficiency, as well as the effects of using V_0.
DE_OVER_E	FLOAT (NOVARY) (32-bit float)	64-element array of energy resolution (FWHM) as a function of energy.
ACCUM_TIME	FLOAT (NOVARY) (32-bit float)	Accumulation time for each sample, nominally 4×1.09 ms to account for the summation over 4 deflection steps for each element of the telemetry product that is used to make the PADs
ENERGY	FLOAT (NOVARY) (32-bit float)	64-element array of energies (eV) covered by the distribution. All 64 energies are provided, even when B = 2 or 4.

PA	FLOAT (32-bit float)	64×16-element array of center pitch angles covered by the distribution. This array varies with each time step as the magnetic field direction changes.
D_PA	FLOAT (32-bit float)	64×16-element array of pitch angle ranges (full width) spanned by each PA bin. This array varies with each time step as the magnetic field direction changes.
G_PA	FLOAT (32-bit float)	64×16-element array of relative sensitivity mapped into pitch angle. Each pitch angle bin maps to one of the 96 solid angle bins of the 3D distribution. The corresponding G_AZIM and G_ELEV for that solid angle bin are multiplied to produce G_PA. This array varies with each time step as the magnetic field direction changes.
B_AZIM	FLOAT (32-bit float)	Magnetic field azimuth in instrument coord., as calculated onboard the spacecraft.
B_ELEV	FLOAT (32-bit float)	Magnetic field elevation in instrument coord., as calculated onboard the spacecraft.
NUM_DISTS	INTEGER (NOVARY) (32-bit signed integer)	Number of PAD distributions in the file

Table 9: Contents for swea.calibrated.svy_spec and swea.calibrated.arc_spec data files

Field Name	Data Type	Description
EPOCH	TT2000 (64-bit signed integer)	UTC time from 01-Jan-2000 12:00:00.000 including leap seconds, one element per energy spectrum (NUM_SPEC elements)
TIME_MET	DOUBLE (64-bit float)	Mission elapsed time (spacecraft clock or SCLK in SPICE terms) for this data record, one element per energy spectrum (NUM_SPEC elements)
TIME_UNIX	DOUBLE (64-bit float)	Unix time (elapsed seconds since 1970-01-01/00:00 without leap seconds) for this data record, one element per energy spectrum (NUM_SPEC elements)
NUM_ACCUM	INTEGER (8-bit signed integer)	Number of two-second accumulations per energy spectrum (NUM_SPEC elements)
COUNTS	FLOAT (32-bit float)	64-element array of counts calculated by summing over all angles in the 3D distributions, one array per energy spectrum (NUM_SPEC×64 elements)

DIFF_EN_FLUX	FLOAT (32-bit float)	64-element array of differential energy fluxes [eV/(cm^2 s sr eV)] computed from the COUNTS array, the full sensor geometric factor GEOM_FACTOR, the accumulation time ACCUM_TIME, and the number of accumulations per distribution NUM_ACCUM, one array per energy spectrum (NUM_SPEC×64 elements)
WEIGHT_FACTOR	FLOAT (NOVARY) (32-bit float)	Weighting factor for converting raw counts to raw count rate.
GEOM_FACTOR	FLOAT (NOVARY) (32-bit float)	Geometric factor per anode [cm^2 s sr eV/eV] measured at 1.4 keV. This includes a factor for the overall MCP efficiency at 1.4 keV.
G_ENGY	FLOAT (NOVARY) (32-bit float)	64-element array of relative sensitivity as a function of energy. This accounts for the energy dependence of the MCP efficiency, as well as the effects of using V_0.
DE_OVER_E	FLOAT (NOVARY) (32-bit float)	64-element array of energy resolution (FWHM) as a function of energy
ACCUM_TIME	FLOAT (NOVARY) (32-bit float)	Accumulation time for each sample, nominally 96×4×1.09 ms to account for the summation over 4 deflection steps for each azimuth-elevation element, then summation over the 16×6 angle elements to make the energy spectrum
ENERGY	FLOAT (NOVARY) (32-bit float)	64-element array of energies (eV) covered by the distribution
NUM_SPEC	INTEGER (NOVARY) (32-bit signed integer)	Number of energy spectra in the file

6.2 Document Product File Formats

Documents are provided in either Adobe Acrobat PDF/A or plain ASCII text format. Other versions of the document (including HTML, Microsoft Word, etc.) may be included as well.

6.3 PDS Labels

PDS labels are ASCII text files written, in the eXtensible Markup Language (XML). All product labels are detached from the digital files (if any) containing the data objects they describe (except Product_Bundle). There is one label for every product. Each product, however, may contain one or more data objects. The data objects of a given product may all reside in a single file, or they may be stored in multiple separate files. PDS4 label files must end with the file extension ".xml".

The structure of PDS label files is governed by the XML documents described in Section 6.3.1.

6.3.1 XML Documents

For the MAVEN mission PDS labels will conform to the PDS master schema based upon the 1.1.0.1 version of the PDS Information Model for structure, and the 1.1.0.1 version of the PDS schematron for content. By use of an XML editor these documents may be used to validate the structure and content of the product labels.

The PDS master schema and schematron documents are produced, managed, and supplied to MAVEN by the PDS. In addition to these documents, the MAVEN mission has produced additional XML documents which govern the products in this archive. These documents contain attribute and parameter definitions specific to the MAVEN mission. A full list of XML documents associated with this archive is provided in Table 7. A list of the XML documents associated with this archive is included in this document in the XML_Schema collection section for each bundle.

Examples of PDS labels required for the SWEA archive are shown in Appendix C (bundle products), Appendix D (collection products), and Appendix E (basic products).

6.4 Delivery Package

Data transfers, whether from data providers to PDS or from PDS to data users or to the deep archive, are accomplished using delivery packages. Delivery packages include the following required elements:

1. The package which consists of a compressed bundle of the products being transferred.
2. A transfer manifest which maps each product's LIDVID to the physical location of the product label in the package after uncompression.
3. A checksum manifest which lists the MD5 checksum of each file included in the package after uncompression.

SWEA archive delivery packages (including the transfer and checksum manifests) for delivery to PDS are produced at the MAVEN SDC.

6.4.1 The Package

The directory structure used in for the delivery package is described in the Appendix in Section F.1. Delivery packages are compressed using either [zip, or tar/gzip] and are transferred electronically using the ssh protocol.

6.4.2 Transfer Manifest

The "transfer manifest" is a file provided with each transfer to, from, or within PDS. The transfer manifest is external to the delivery package. It contains an entry for each label file in the package, and maps the product LIDVID to the file specification name for the associated product's label file. Details of the structure of the transfer manifest are provided in Section F.2.

The transfer manifest is external to the delivery package, and is not an archive product. As a result, it does not require a PDS label.

6.4.3 Checksum Manifest

The checksum manifest contains an MD5 checksum for every file included as part of the delivery package. This includes both the PDS product labels and the files containing the digital objects which they describe. The format used for a checksum manifest is the standard output generated by the md5deep utility. Details of the structure of the checksum manifest are provided in section F.3.

The checksum manifest is external to the delivery package, and is not an archive product. As a result, it does not require a PDS label.

Appendix A Support staff and cognizant persons

Table 10: Archive support staff

SWEA team			
Name	**Address**	**Phone**	**Email**
David L. Mitchell	Space Sciences Laboratory, 7 Gauss Way, University of California, Berkeley, CA 94720	+001 510-643-1561	mitchell@ssl.berkeley.edu
Matt Fillingim	Space Sciences Laboratory, 7 Gauss Way, University of California, Berkeley, CA 94720	+001 510-643-8485	matt@ssl.berkeley.edu

UCLA			
Name	**Address**	**Phone**	**Email**
Dr. Steven Joy PPI Operations Manager	IGPP, University of California 405 Hilgard Avenue Los Angeles, CA 90095-1567 USA	+001 310 825 3506	sjoy@igpp.ucla.edu
Mr. Joseph Mafi PPI Data Engineer	IGPP, University of California 405 Hilgard Avenue Los Angeles, CA 90095-1567 USA	+001 310 206 6073	jmafi@igpp.ucla.edu

Appendix B Naming conventions for MAVEN science data files

This section describes the naming convention used for science data files for the MAVEN mission.

Raw (MAVEN Level 0):

mvn_<inst>_<grouping>_l0_< yyyy><mm><dd>_v<xx>.dat

Level 1, 2, 3+:

mvn_<inst>_<level>_<descriptor>_<yyyy><mm><dd>T<hh><mm><ss>_v<xx>_r<yy>.<ext>

Table 19: File naming convention code descriptions.

Code	Description
<inst>	3-letter instrument ID
<grouping>	Three-letter code: options are all, svy, and arc for all data, survey data, and archive data respectively. Primarily for PF to divide their survey and archive data at Level 0.
<yyyy>	4-digit year
<mm>	2-digit month, *e.g.* 01, 12
<dd>	2-digit day of month, *e.g.* 02, 31
<hh>	2-digit hour, separated from the date by T. OPTIONAL.
<mm>	2-digit minute. OPTIONAL.
<ss>	2-digit second. OPTIONAL.
v<xx>	2-digit major revision number: For Level 0 data: increments whenever Level 0 data are reprocessed, typically to complete partial days or to fill in data gaps. For Level 1, 2, 3+ data: increments with a significant change in the processing algorithm or instrument calibration parameters. Typically triggers reprocessing of the entire data set.
r<yy>	2-digit minor revision number: increments whenever the data are regenerated without a change to the major revision. This can occur for a variety of reasons, typically to fill in missing science data or to apply new or updated ancillary data, such as SPICE kernels.
<descriptor>	A description of the data. Defined by the creator of the dataset. There are no underscores in the value.
<ext>	File type extension: fits, txt, cdf, png
<level>	A code indicating the MAVEN processing level of the data (valid values: l1, l2, l3). See Section 3.1, Table 8, for level definitions.

Either all elements of the optional T<hh><mm><ss> field will be present, or all will be omitted. If omitted, the data within the file span one UT day, with time tags ranging from 00:00:00 to 23:59:59. Data do not necessarily start at 00:00:00 or end at 23:59:59, and data gaps may occur within the file.

Table 20: File naming convention instrument codes.

Instrument name	**<instrument>**
IUVS	iuv
NGIMS	ngi
LPW	lpw
MAG	mag
SEP	sep
SWIA	swi
SWEA	swe
STATIC	sta
PF package	pfp

Appendix C Sample Bundle Product Label

This section provides a sample bundle product label.

Appendix D Sample Collection Product Label

This section provides a sample collection product label.

Appendix E Sample Data Product Labels

This section provides sample product labels for the various data types described in this document.

Appendix F PDS Delivery Package Manifest File Record Structures

The delivery package includes two manifest files: a transfer manifest, and MD5 checksum manifest. When delivered as part of a data delivery, these two files are not PDS archive products, and do not require PDS labels files. The format of each of these files is described below.

F.1 Transfer Package Directory Structure

[Insert a description of the directory structure contained in the delivery package.]

F.2 Transfer Manifest Record Structure

The transfer manifest is defined as a two field fixed-width table where each row of the table describes one of the products in the package. The first field defines the LIDVID of each product in the package. The second field defines the file specification name of the corresponding product label in the package. The file specification name defines the name and location of the product relative to the location of the bundle product.

F.3 Checksum Manifest Record Structure

The checksum manifest consists of two fields: a 32 character hexadecimal (using lowercase letters) MD5, and a file specification from the root directory of the unzipped delivery package to every file included in the package. The file specification uses forward slashes ("/") as path delimiters. The two fields are separated by two spaces. Manifest records may be of variable length. This is the standard output format for a variety of MD5 checksum tools (*e.g.* md5deep, etc.).